# ACTIVE NOISE ATTENUATION

by

WILLIAM RHUEL SHORT

S.B., Massachusetts Institute of Technology
(1973)

M.S., Massachusetts Institute of Technology
(1975)

SUBMITTED IN PARTIAL FULFILLMENT
OF THE REQUIREMENTS FOR THE
DEGREE OF

DOCTOR OF SCIENCE

at the

MASSACHUSETTS INSTITUTE OF TECHNOLOGY
February, 1980



Signature redacted

Signature of Author.....
Department of Electrical Engineering and Computer Science,
February, 1980

Signature redacted

Certified by.....
Amar G. Bose
Thesis Supervisor

Signature redacted

Accepted by.....
Arthur Smith
Chairman, Departmental Graduate Committee

# ACTIVE NOISE ATTENUATION

by

WILLIAM RHUEL SHORT

Submitted to
the Department of Electrical Engineering and Computer Science
on November 14, 1979, in partial fulfillment of the
requirements for the Degree of Doctor of Science.

## ABSTRACT

A new method for slobally reducing the amount of unwanted power radiated by acoustic sources, by means of active devices, is proposed. After examining previously reported passive and active noise attenuating techniques, and finding them to be unsuitable for some applications, a new method is proposed. The scheme involves placing an attenuating source close to the noise source, driven in such a way as to form a dipole out of the two sources, thus reducing the acoustic power radiated.

Equations are derived relating the total power radiated to the volume velocities of acoustic point sources. Beginning with the simplest case, that of a single attenuating source, a system is derived which produces the required volume velocity at the attenuating source, and an electrical model of this system is created. The model is used to verify system stability and to predict the amount of noise reduction that may be obtained. A laboratory realization of the system is constructed having performance closely matching that of the model. When tested under ideal conditions, the system provides 16 db of noise reduction, within 2 db of the calculated theoretical maximum. For typical noise sources, the reduction drops to 8 db.

The need for multiple noise attenuating loops is discussed. Equations are derived predicting the performance of such a system. A computer model is built to answer questions of stability and performance. A laboratory system is constructed which verifies the computer model. A second attenuating loop increases the noise reduction from 8 to 12 db for one typical noise source.

Thesis supervisor: Prof. Amar G. Bose, Professor of Electrical Engineering.

## ACKNOWLEDGEMENTS

The author wishes to acknowledge the assistance of several people whose help throughout the course of this work proved instrumental in its completion.

Prof. A. G. Bose, the thesis supervisor. The original concept for the device described in this thesis was his and was the outgrowth of some previous work done by him at Bose Corporation in this area. His guidance through the years required to complete the work described in this thesis was of immeasureable help. His ability to point the student to the area where concentrated effort would provide the greatest return greatly reduced the time spent exploring dead-end avenues.

Prof. K. N. Stevens and Prof. L. A. Gould, the thesis readers. Both of these gentlemen were able to provide useful criticism not only in their fields of expertise, but also on a wide variety of topics germane to the work. Their discussions and encouragement were of enormous help throughout.

Mr. J. C. Carter. While engaged in research on a related topic at Bose Corporation, he broke ground in a number of areas essential to this thesis. His discussion was

invaluable in making this project work.

The people of Bose Corporation. Some of the work described in this thesis was performed using equipment and facilities of the Bose Corporation. Without the cooperation of these people, this work would have been impossible.

Finally, the author wishes to acknowledge the work of Dr. Arthur C. Clarke, who had the foresight to predict a global noise reducing device in his short story, "Silence Please" published in 1950. The story humorously discusses the social effects of the use of such a device, and while not completely accurate on technical matters, it does suggest a number of novel uses for such a device.

TABLE OF CONTENTS

# Chapter 1

## INTRODUCTION

As a result of the explosion in the uses and numbers of machines in this Industrial Age, people have been plagued by unwanted acoustical energy in the environment, both indoors and out. Only in this century have the necessary scientific and engineering disciplines been developed sufficiently to allow control of this noise energy. Yet, noise continues to be a serious problem, not only in the working environment, but in the home environment as well. The art of controlling noise has not kept pace with the demand for better noise control. Legislated limits to noise exposure continue to become tighter in order to better protect the populace, but noise control schemes have generally remained the same.

Noise exposure has many detrimental effects on humans. It can cause mental fatigue and discomfort, and, over a period of time, can increase hearing threshold levels, resulting in all the discomforts, costs, and inconveniences associated with hearing loss.

In the course of a day, one can easily observe a variety

of locations where noise reduction could be beneficially applied. In the typical city environment, traffic noise (both wheel rumble and engine exhaust noise), could be reduced. In the typical home or apartment, noise from appliances, or from adjoining rooms or residences can be objectionable, and might be amenable to better noise control. In the workplace, the application of noise control would be of great benefit for silencing a wide variety of machines--from machine tools to air compressors.

Despite the wide variety of opportunities to apply noise control, the state of the art is not very advanced. Typically, passive elements are used for noise control. Although these methods work in a satisfactory manner at mid and high frequencies, at low frequencies they require an inordinate amount of mass in order to do an effective job. Such passive devices for low frequency noise attenuation are bulky, costly, and difficult to apply.

Since passive methods seem incapable of satisfactorily reducing low frequency noise, an active method should be investigated. Such a system might include a microphone or an array of microphones, a loudspeaker, or an array of loudspeakers, plus associated electronics for signal processing. An active system might be developed having lower cost, lower mass, and greater ease of use than a passive system with similar reduction. Since passive methods are capable of mid and high frequency attenuation, then it would

seem reasonable to confine the examination of active systems to low frequencies. Besides being better able to compete with passive systems at these frequencies, the associated processing electronics are likely to be much simpler at low frequencies than high, due to the lower phase shift associated with time delays in the system at low frequencies.

The discussion below will show that reasonable passive methods are not capable of adequately supressing noise at low frequencies. Some active methods of noise control which have been reported in the literature will be examined, but these methods will also be shown to be inadequate for various reasons. A new method of globally reducing noise radiated from a localized noise source through the use of a closed loop system containing acoustical, mechanical, and electrical elements will be proposed. The theoretical limitations of such a system will be examined, followed by an examination of the practical limitations. Finally, the practical limits will be verified experimentally.

# Chapter 2

# PREVIOUSLY REPORTED NOISE CONTROL METHODS

## I. PASSIVE METHODS

A widely used method for reducing unwanted acoustic energy is through the use of passive devices. These passive devices may be used to reduce the amount of acoustic energy put out by the source, or they may attenuate the energy after it has been generated as it propagates through the air or through solid members directly connected to the noise source.

In a number of industries, studies have been made of particular machines in order to reduce the noise generated by those machines. Examples include the study and redesign of noisy gear trains in some machines, and the redesign of particularly noisy rotating or reciprocating members. This redesign can significantly reduce the amount of noise generated by the machine and reduce the difficulty of externally quieting the machine. An inspection of the Patent Review section of the Journal of the Acoustical Society of America will usually turn up several patents each month for passive noise attenuators applied to specific machines.

If, as is usually the case, machine redesign can not sufficiently quiet the noise, noise reduction must be applied external to the source. Such an application is not without its problems, however.

Consider a model for a typical passive noise suppression system, shown in figure 2-1.

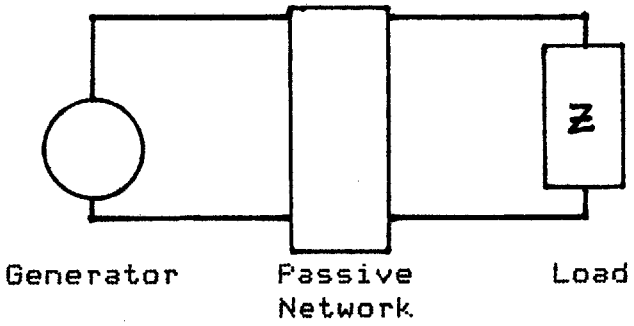


Figure 2-1. Passive attenuator model.

A source of noise, modeled by the generator, is to be connected to the listening environment, modeled by the impedance, through some network of passive elements. This network should be designed to prevent energy transfer from the source to the load at frequencies of interest.

However, mechanical and acoustical circuits are constrained by the fact that mass elements must be referenced to ground. In an electrical model of acoustic or mechanical circuits, all masses, which are represented by capacitors, must have one end connected to ground, as discussed in Beranek (1). This constraint limits the types of filters that can be constructed.

A typical filter might be modeled using lumped parameter elements as shown in figure 2-2.

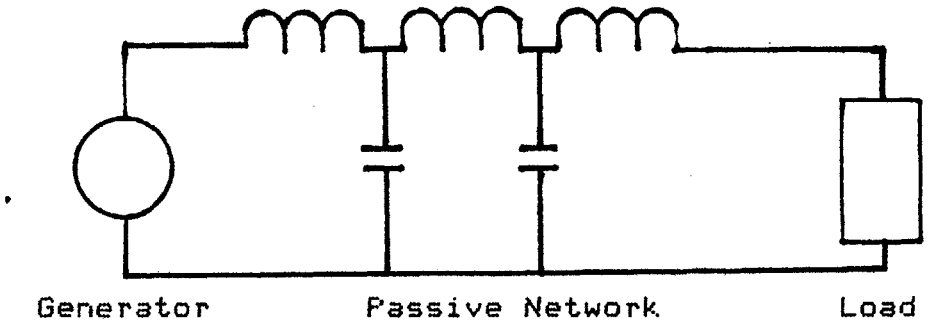


Figure 2-2. Passive attenuator model.

The generator is connected to the source through a series of compliances and masses. Neglecting damping for the moment, the frequency below which the filter is no longer effective in reducing energy transmitted is proportional to the reciprocal of the square root of the product of the mass and the compliance. If the desire is to reduce noise propagation at low frequencies, either the compliance must be increased, resulting in a weak, flexible mechanical structure, or the mass must be increased.

Herein lies the problem with reducing noise transmission using passive structures. The only practical way to attenuate airborne low frequency noise passively is to use large masses. Large masses tend to be bulky, expensive, and, obviously, heavy. Such attenuators are inconvenient to use in many applications.

As an example, suppose a noise reduction of 20 db at 50

Hz is desired. If a single walled, solid, damped partition is used to enclose the noise source, figure 10-26 in Beranek (1) shows that a surface density of 14 pounds/square foot is required. Thus, a partition made from one inch thick aluminum walls, or from one quarter inch thick lead walls would be needed to give the required attenuation.

If the noise source is contained within a two foot cube, then 336 pounds of material are required to obtain the desired noise attenuation. Such a weight would preclude this noise attenuator from being used in any portable application. And even a small hole or leak in the partition would greatly diminish the noise attenuation, so the structure must completely seal the noise source, eliminating any access to it and eliminating the possibility of ventilating it. At current prices, the required aluminum stock would cost approximately $700. And, if one wanted to decrease the cutoff frequency by an octave to 25 Hz, the weight would quadruple to over half a ton, and the price of materials would increase to nearly $3000. Additionally, this noise attenuator would only quiet a machine enclosed in its small two foot cube volume. Finally, the equation taken from Beranek used in calculating these figures contains some approximations and assumptions and yields a result which is indicative of the best performance one could expect. Typically, one would not obtain as great a noise reduction as that calculated using this formula.

Noise reduction may also be achieved through the use of acoustic resistances which absorb energy. However, large quantities of materials are required in order to obtain significant low frequency attenuation. For example, in order to achieve 20 db of attenuation at 50 Hz, Beranek (1) shows that 80 feet of 4 inch thick fiberglass baffles located on 8 inch centers are required.

If the noise energy is predominately at one frequency, an acoustic resonator could be used to reduce the noise level at that frequency. However, such a structure would be large, due to the high compliance, and thus large volume required.

The effectiveness of passive attenuation systems can be improved by using multiple walled systems with air gaps. However, it is easy to see that if significant noise reduction at low frequencies is required, passive systems are simply too expensive, too heavy, and too inconvenient. The importance of controlling low frequency noise should not be underestimated. Tempest (30) showed that noise below 100 Hz was annoying far in excess of what its A weighted level would predict. So, there exists a need to reduce low frequency noise which passive systems can not fulfill.

## II. OPEN LOOP ACTIVE METHODS

Since passive methods have been shown to be unsatisfactory for attenuating low frequency noise, active

methods need to be investigated. The first reference to the use of active methods to reduce unwanted sound seems to be a patent granted to Lueg (17) in 1936. A search of the literature shows that more recently, two approaches have been used: open loop methods, in which the amount of attenuation is not monitored by the system, and closed loop methods, where feedback is utilized, so that noise reduction is constantly optimized by the system.

Typically, the open loop systems divide space into two regions, as shown in figure 2-3.

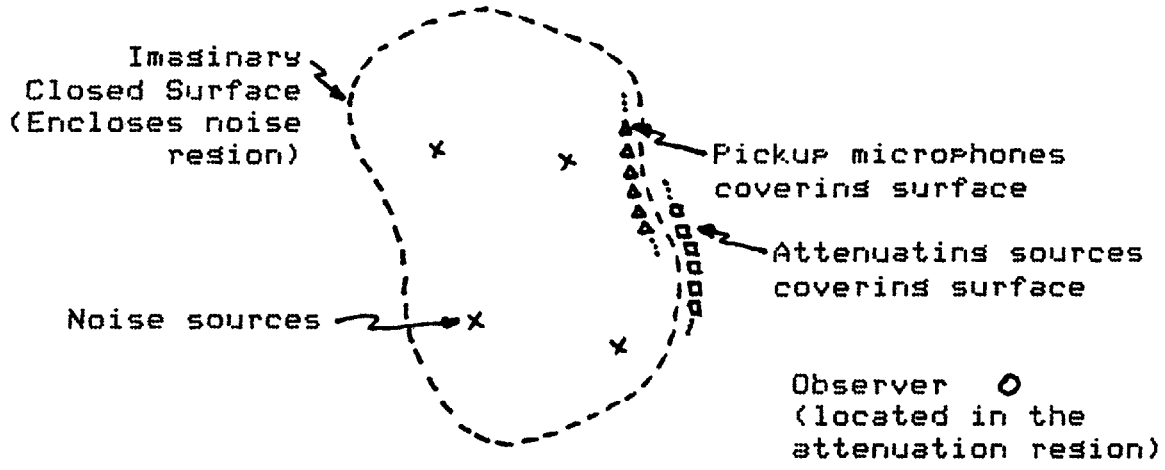


Figure 2-3. Attenuation by Huygens' Sources.

One region contains the noise sources, and the other contains the listeners. It is in this second region that noise attenuation is desired. Separating these two regions is an imaginary closed surface. On this surface are placed the

devices which produce the noise reduction.

Such a system relies on Huygens' principle, better known in optics, but here applied to acoustics. The principle states that a wavefront produced by a primary source may also be considered as the sum of wavefronts produced by an infinite number of simple secondary sources. In noise attenuation devices, the acoustic sources on the closed surface act as the secondary sources referred to by Huygens. The noise sources, which are the primary source, are enclosed by the surface, and create some wavefront on the surface. If the secondary attenuating sources on the surface are appropriately driven, they can sum to create a wavefront having the same magnitude but opposite sign to that generated by the primary noise sources. Thus, in the region outside the surface, the two wavefronts sum to zero, and the noise sources enclosed by the surface are quieted.

This approach to the problem has been used by a number of investigators, particularly in France and the Soviet Union. Mangiante (18), and Canevet and Mangiante (4) in particular, along with Jessel and Mangiante (12) and Fedoryuk (10), have investigated the types of sources required on the surface for optimal noise attenuation. Jessel and Mangiante (12) determined that the required sources are directional, with a cardioid pattern. This pattern is generated using "tripole" sources, each consisting of a dipole source and a monopole source. The sources are oriented so that they

radiate maximum power to the outside region of space. They are driven by signals derived from the pressure as measured just inside the surface. The pressure measurement is made using tripole microphones lying inside the surface in the region of the noise sources, and sensitive only in the direction of the noise sources. Since the attenuating sources put out sound only in the noise attenuation region, and since the pressure microphones pick up sound only from the noise source region, the microphones are insensitive to the output of the noise attenuating sources, and the system operates in an open loop manner.

Mangiante (18) investigated the problems encountered when the infinite number of attenuating sources required to cover the imaginary surface are replaced with a finite number of sources. This constraint limits the amount of noise reduction and the bandwidth over which reduction may be obtained.

Mangiante (18) experimentally examined this technique. Twenty attenuating sources were located on a 0.8m diameter imaginary sphere. Twelve noise sources were located on a concentric 0.2m sphere. A far field reduction in sound pressure level of 15 to 30 db was obtained for sine waves in the range of 250 to 500 Hz, and a reduction of 10 to 15 db for narrow band noise was measured in this same frequency range. The experiment was conducted in an anechoic chamber. However, the signals fed to the attenuating sources were not

derived from a microphone pickup, but from the actual signal exciting the noise sources. In practice, the fact that a finite number of microphones would be used would tend to decrease the amount of attenuation obtainable.

In air ducts, it is possible to treat the problem one dimensionally. The duct is divided by an imaginary plane normal to the air flow through which all air must flow. If the noise sources are assumed to be upstream of this plane, then the noise source region may be considered to be the region upstream of this plane and the noise attenuation region to be downstream. Canevet (3) and Canevet and Mansiante (4) used this approach and studied noise reduction in air ducts. Acoustic waves were introduced by means of a loudspeaker into one end of a duct, 8cm in diameter and 3m long. Halfway down the duct, a tripole source was arranged, beaming downstream, fed by a signal derived from the electrical signal driving the noise source loudspeaker. Upstream from the attenuating source, no change in sound pressure was reported by Canevet and Mansiante (4), but downstream, a 50 to 70 db drop in level was observed for sine waves. Since the system was operating in an open loop manner, this reduction was critically sensitive to temperature changes and drift in the electronics. Canevet (3) refined the system by using better tripole sources driven by an upstream microphone. Downstream, noise was reduced by 40 db for sine waves and 15 db for narrow band noise.

Swinbanks (27) examined the one dimensional problem and calculated that attenuations of up to 50 db were possible over a wide range of frequencies. Instead of using tripole sources, Swinbanks determined that a unidirectional plane wave source made up of a small number of simple sources on the surface of the duct could produce this degree of attenuation. A similar arrangement of microphones upstream could detect the oncoming noise wavefront. Poole and Leventhall (23) experimentally verified this technique and reported 50 db of noise reduction for sine waves.

Other open loop techniques have been reported for use in situations where the noise waveform is sufficiently well known that pickup microphones are unnecessary. Conover (6) and Hawley (11) have both discussed systems in which the attenuating sources are driven from a signal derived from the electrical signal which excites the noise source. Such a system could be used only where the noise is generated by a device excited by a known electrical signal. Conover (6) described such a system which was tested using a high power electrical transformer. Transformers and similar electrical apparatus are excited by the 60 Hz current flowing through them and typically generate acoustical energy at frequencies of 120 Hz and harmonics of 120 Hz.

Conover placed a single loudspeaker next to a 15000 KVA transformer. A microphone was placed 30 to 60 feet away, on axis in the far field, to monitor the amount of noise attenu-

ation obtained. The speaker was fed with sine waves at 120, 240, and 360 Hz, of adjustable amplitude and phase. The amplitude and phase of each frequency sine wave was manually adjusted to minimize the sound pressure as measured by the far field monitor microphone. A polar plot of noise attenuation was then made. 20 db of attenuation was reported on axis, but for most angles, significantly less attenuation was recorded. And, for many angles, increased sound pressure was measured. However, due to the changing nature of the electrical load on the transformer and the changing weather conditions, the signal driving the attenuating source had to be adjusted frequently, by as much as 6 db per hour, to maximize noise attenuation.

One can clearly see the disadvantage of the open loop systems thus far reported. Once the noise attenuation system is set up and optimized, performance is degraded by changes in the system which are certain to occur. Thus, in most applications, an open loop system does not suffice, and a more complex system is required.

## III. CLOSED LOOP ACTIVE METHODS

Since open loop methods lack the ability to adjust to meet changing conditions, the application of feedback to active noise attenuation methods should be considered. By utilizing feedback, the system can be made to monitor its own

performance, and the effects of changing operating conditions can be minimized.

Several schemes have been reported in which closed loop techniques were used for reducing vibration in solid objects such as beams or plates. Papers by Tartakowski (29), Knyasev and Tartakowski (13, 14), and Rockwell and Lawther (25) have discussed the use of feedback to reduce vibration at audio frequencies. These systems typically measure the velocity or force at a point or array of points on the beam or plate and use a feedback loop with a velocity or force transducer to minimize the disturbance measured. By setting the velocity of a point on a beam to zero, Rockwell and Lawther (25) reported a reduction of 30 db in vibration level over a wide range of frequencies.

These systems have practical uses as noise abatement devices in locations where sound transmission along solid members, such as a beam or a plate, is a problem. For example, if such a system were applied to a mounting plate for a piece of heavy machinery, less noise would be transmitted to the floor, and the overall noise level in the room would be decreased.

An additional type of closed loop noise attenuation system also exists. Such a system reduces airborne noise as it travels from the noise source to the listener, using closed loop techniques. However, little has been reported in the literature on such a system. Olson (20, 21) and

coworkers at RCA wrote about such a system in the early 50's. Their system attempts to minimize the sound in a region around a point due to a distant noise source. This minimization is accomplished by using a feedback system to set the incremental pressure of a point to zero. If any theoretical work was done to determine the desirability of this approach to the problem, it was not reported. Figure 2-4 shows a schematic representation of the system.

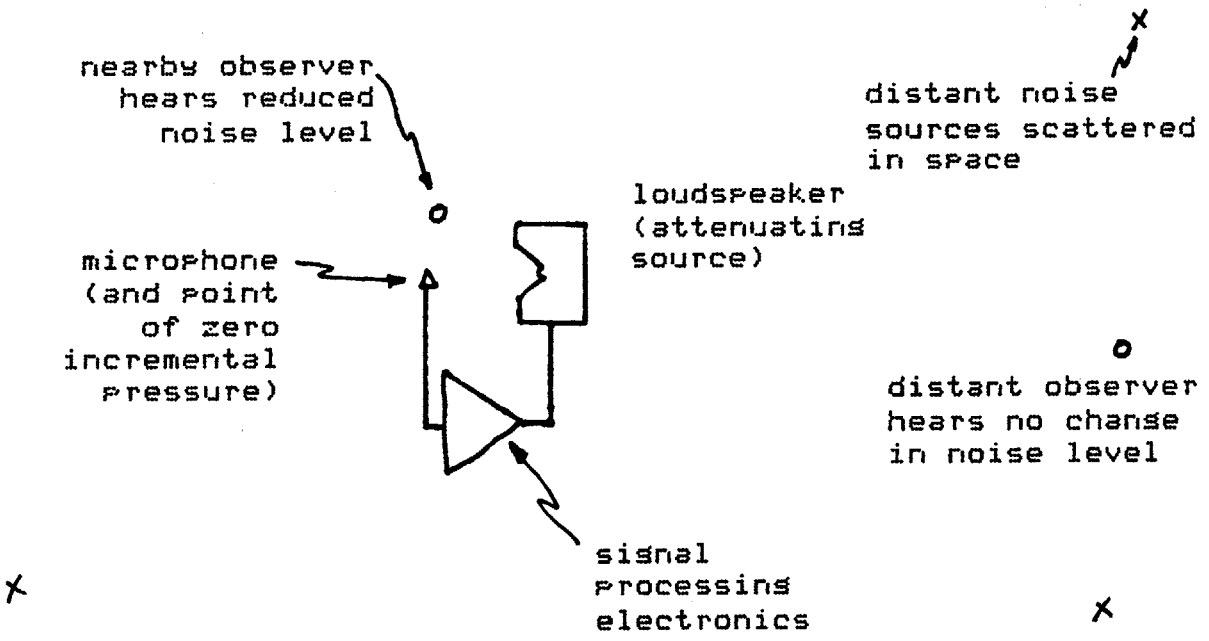


Figure 2-4. Olson's active noise attenuation system.

A microphone is placed in close proximity to a loudspeaker. The microphone feeds electronic circuitry containing a high gain amplifier, compensation electronics, and a power amplifier, which drives the speaker. This system forces the

incremental pressure at the microphone to become close to zero for frequencies at which the loop operates. As a result, an observer close to the microphone would hear a reduction in noise from a distant noise source.

Olson (20) used an especially desisned loudspeaker and microphone which were separated by a distance of approximately one inch. The system decreased the sound pressure level at the microphone due to distant noise sources by a maximum of 25 db, over a ranse from 20 to 200 Hz. Four inches from the microphone, the maximum attenuation dropped to 15 db, and at ten inches away from the microphone, maximum attenuation became 12 db.

Since this technique works only when the listener and microphone are separated by a small fraction of a wavelensth of sound, the device quiets only a small volume of space directly around the microphone. However, even with this limitation, the system can be useful. Simshauser and Hawley (26) proposed that this technique be used in noise reducins headsets, which could provide better ear protection than passive headsets in noisy environments. They reported that as much as 15 db of attenuation could be obtained at low and midband frequencies.

While these techniques are capable of providins significant noise attenuation, they do so only over a limited volume of space. There remained a need for a system which would allow slobal noise reduction when a noise attenuatins device

was applied locally to a noise source. It was from this point that new work on the problem of active noise attenuation began.

# Chapter 3

# A GLOBAL NOISE ATTENUATION METHOD

The proposed device would operate in a different manner than those previously described in the literature. It would be placed close to a noise source, and would actively process and modify the noise generated by the noise source in such a way as to reduce the total power radiated by the combination of the noise source and attenuating source when compared to the noise source operating alone.

The general form that such a device would take is shown schematically in figure 3-1. A microphone is placed close to both a noise source and an attenuating source, which could be a loudspeaker. As will be shown below, if the attenuating source is forced to have the same magnitude of volume velocity as the noise source, but with opposite sign, then the noise source and attenuating source effectively become a dipole source, and the total power radiated is reduced. This situation may be obtained by suitable design of the signal processing electronics. The power reduction occurs only for frequencies where the separation between the noise source and

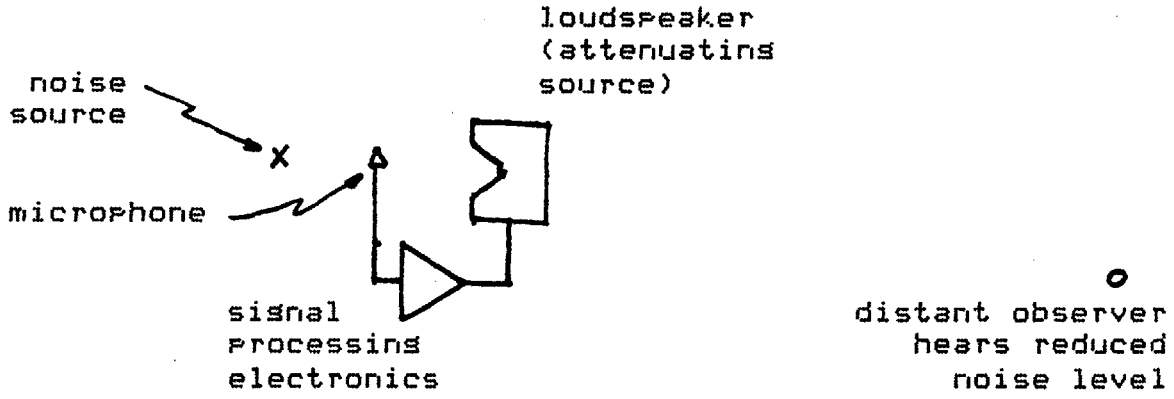


Figure 3-1. Proposed attenuation system. Microphone, noise source, and loudspeaker are all closely spaced.

the attenuating source is small compared to a wavelength of sound. Therefore, for low frequencies, the sound pressure level heard by a distant observer is much less for the combination of noise and attenuating sources than for the noise source alone.

At higher frequencies, where the separation between the noise source and the attenuating source becomes comparable to, or large compared to the wavelength of sound, no sound attenuation can be expected. Stability constraints on the feedback loop, however, require that the system gain be low, and thus the output of the attenuating source is also be low at these frequencies. As a result, the noise attenuator has little effect on the overall noise level at high frequencies. This limitation need not be a problem in practical applications, since sound at these frequencies can be

satisfactorily attenuated by passive devices.

This type of device is capable of reducing the total power radiated at low frequencies by noise sources small compared to a wavelength of sound. For noise sources comparable to or larger than a wavelength, several such attenuating sources are required.

First, the form of the noise attenuation device must be examined. The simplest possible problem is that of a simple point noise source and a simple point attenuating source. If the position and volume velocity of the noise source are known, then it should be possible to determine a position and volume velocity for the attenuating source which minimizes power radiated.

In order to undertake this problem, an expression for the power radiated by two point sources which are closely spaced compared to a wavelength must first be derived. The geometry of the problem is shown in figure 3-2. The noise source is located at the origin, and has volume velocity $\underline{Vvn}$, with a magnitude Vvn and zero phase angle. (Throughout this paper, the convention that underlined variables represent complex quantities will be used.) The attenuating source is located at a point $(r_c, \theta_c)$ in polar coordinates, and has volume velocity $\underline{Vvc}$, of magnitude Vvc and phase $\psi$.

The distance from the origin, and thus from the noise source, to a distant observer is represented by r. Making the assumption that r is sufficiently large compared to $r_c$,

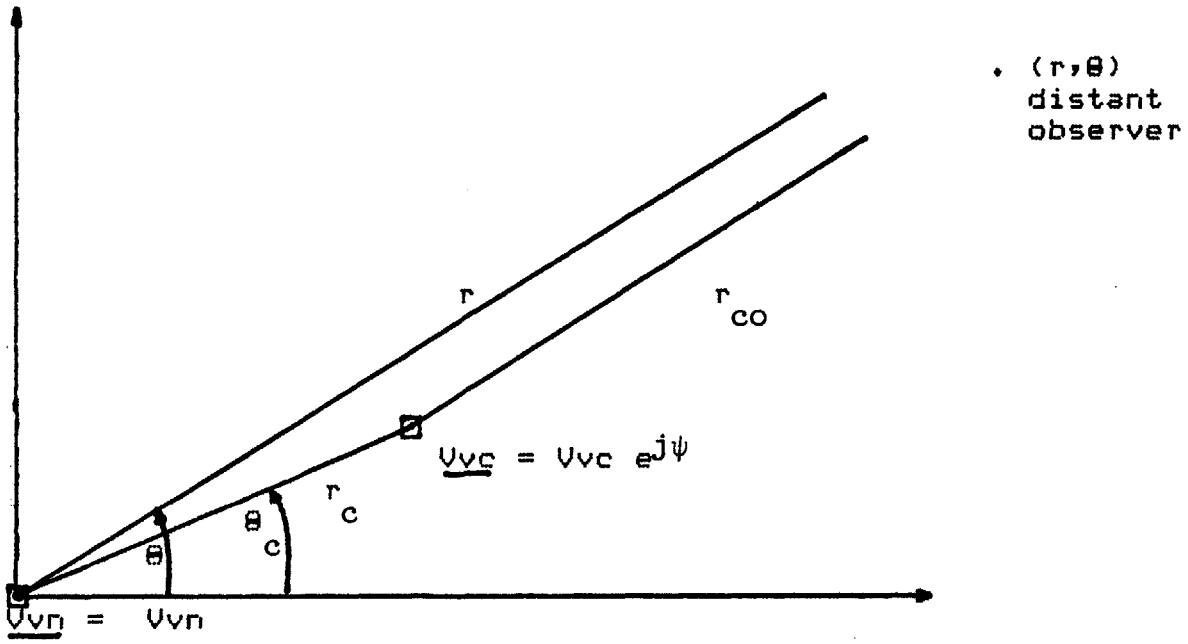


Figure 3-2. Geometry of the two point source attenuation problem. Noise source with volume velocity Vvn is located at the origin, and attenuating source with volume velocity Vvc is located at $(r_c, \theta_c)$.

the distance from the attenuating source to the noise source, so that r and $r_{co}$ are nearly parallel, then the distance from the attenuating source to the observer can be written

$$r_{co} = r - r_c(\cos(\theta - \theta_c)) \qquad (3.1)$$

The pressure due to a point source having volume velocity Vv and phase $\psi$ is (Beranek's (1) equation 4-3)

$$p(r) = j \frac{Vv\ f\ \rho_o}{2\ r} \exp(-jkr + j\psi) \qquad (3.2)$$

where f is the frequency, $\rho_o$ is the density of air, and k is the wavenumber. Superposition may be used to write the far field pressure due to the noise source and attenuating source as

$$\underline{p}(r) = \frac{j\, Vvc\, f\, \rho_o}{2\, r_{co}} \exp(-jkr_{co} + j\psi) + \frac{j\, Vvn\, f\, \rho_o}{2\, r} \exp(-jkr) \qquad (3.3)$$

Again, making the assumption that r is large compared to $r_c$, $r_{co}$ may be replaced by r in the denominator. Regrouping terms gives

$$\underline{p}(r) = \frac{j\, f\, \rho_o}{2\, r} \exp(-jkr)\{ Vvn + Vvc \exp(j(\psi + kr_c \cos(\theta-\theta_c)))\} \qquad (3.4)$$

In order to find the total power, the magnitude squared of the pressure is needed. It may be written

$$|\underline{p}|^2 = \frac{f^2\, \rho_o^2}{4r^2}\{(Vvn + Vvc \cos(\psi+kr_c\cos(\theta-\theta_c)))^2 + (Vvc \sin(\psi+kr_c\cos(\theta-\theta_c)))^2\} \qquad (3.5)$$

By making the substitution

$$\alpha = \psi + kr_c \cos(\theta-\theta_c) \qquad (3.6)$$

and obtaining

$$|\underline{p}|^2 = \frac{f^2\rho_o^2}{4r^2} (Vvn + Vvc \cos\alpha)^2 + (Vvc \sin\alpha)^2 \qquad (3.7)$$

the expression reduces to

$$|\underline{P}|^2 = \frac{f^2 \rho_o^2}{4r^2} (Vvn^2 + Vvc^2 + 2\, Vvc\, Vvn \cos\alpha) \quad (3.8)$$

The total power radiated, P, by this combination of sources is proportional to the integral of the magnitude squared of the pressure, evaluated over a surface enclosing the two sources.

$$P \propto \int_0^{\pi} \int_0^{2\pi} |\underline{P}|^2 r^2 \sin\phi \, d\theta \, d\phi \quad (3.9)$$

Since the magnitude squared of the pressure is not a function of $\phi$, the integral becomes

$$P \propto r^2 \int_0^{2\pi} |\underline{P}|^2 \, d\theta \quad (3.10)$$

Substituting in the expression for pressure gives

$$P \propto r^2 \int_0^{2\pi} \frac{f^2 \rho_o^2}{4r^2} \{Vvn^2 + Vvc^2 + 2\, Vvc\, Vvn \cos\alpha\} d\theta \quad (3.11)$$

which reduces to

$$P \propto \int_0^{2\pi} \{Vvn^2 + Vvc^2 + 2\, Vvc\, Vvn \cos\alpha\} d\theta \quad (3.12)$$

The problem now becomes one of integrating the expression for the square of the pressure magnitude with respect to theta. This integration may be done term by term. The first two terms are trivial.

$$\int_0^{2\pi} (V_{vn}^2 + V_{vc}^2)\, d\theta = 2\pi\, (V_{vn}^2 + V_{vc}^2) \qquad (3.13)$$

The second term is of the form: $\cos(\cos\theta)$

$$\int_0^{2\pi} 2\, V_{vc}\, V_{vn} \cos(\psi + kr_c \cos(\theta-\theta_c))\, d\theta \qquad (3.14)$$

This integral can be rewritten as

$$2\, V_{vc}\, V_{vn} \int_0^{2\pi} \{\cos\psi \cos(kr_c \cos(\theta-\theta_c))$$

$$+ \sin\psi \sin(kr_c \cos(\theta-\theta_c))\}d\theta \qquad (3.15)$$

Fortunately, because of the requirement that the two point sources be closely spaced in terms of wavelengths, the term $kr_c$ will be small at frequencies of interest. Thus, the cosine term may be expanded in a series

$$\cos(kr_c \cos(\theta-\theta_c)) = 1 - \frac{k^2 r_c^2 \cos^2(\theta-\theta_c)}{2} + \ldots \qquad (3.16)$$

and the sine term, similarly,

$$\sin(kr_c \cos(\theta-\theta_c)) = kr_c \cos(\theta-\theta_c) + \ldots \qquad (3.17)$$

Dropping the higher order terms, the integral becomes

$$2\, V_{vc}\, V_{vn} \cos\psi \int_0^{2\pi} \{1 - \frac{k^2 r_c^2 \cos^2(\theta-\theta_c)}{2}\}d\theta$$

$$+ \sin\psi \int_0^{2\pi} kr_c \cos(\theta-\theta_c)\, d\theta \qquad (3.18)$$

which reduces to

$$2\ Vvc\ Vvn\ \cos\psi\ (2\pi - \frac{\pi\ k^2 r_c^2}{2}) \qquad (3.19)$$

The final result is a proportionality for total power radiated, P, of the form

$$P \propto Vvn^2 + Vvc^2 + Vvc\ Vvn\ \cos\psi\ (2 - \frac{k^2 r_c^2}{2}) \qquad (3.20)$$

From this expression, one can see that power radiated decreases as the spacing between the two sources decreases, as their volume velocity magnitudes become more alike, and as their phase difference more closely becomes 180 degrees. In the situation where the spacing becomes zero, and the volume velocities become identical with a 180 degree phase shift, then the total power radiated becomes zero.

Standard minimization techniques show, as expected, that the more the two sources become like a dipole, the less power is radiated by the pair. This minimization can be confirmed, and a determination made of how much power reduction can be expected by using a computer simulation. Figure 3-3 shows the reduction in power radiated for two point sources. Zero db is the level of the power radiated by a single point source having volume velocity magnitude 1 and phase 0. In generating these curves, the noise point source was set to Vvn = 1, and phase = 0. The attenuating point source had a variable magnitude and phase, as shown on the plot. The sources were located one twentieth of a wavelength apart. Note that maximum attenuation occurs for the dipole

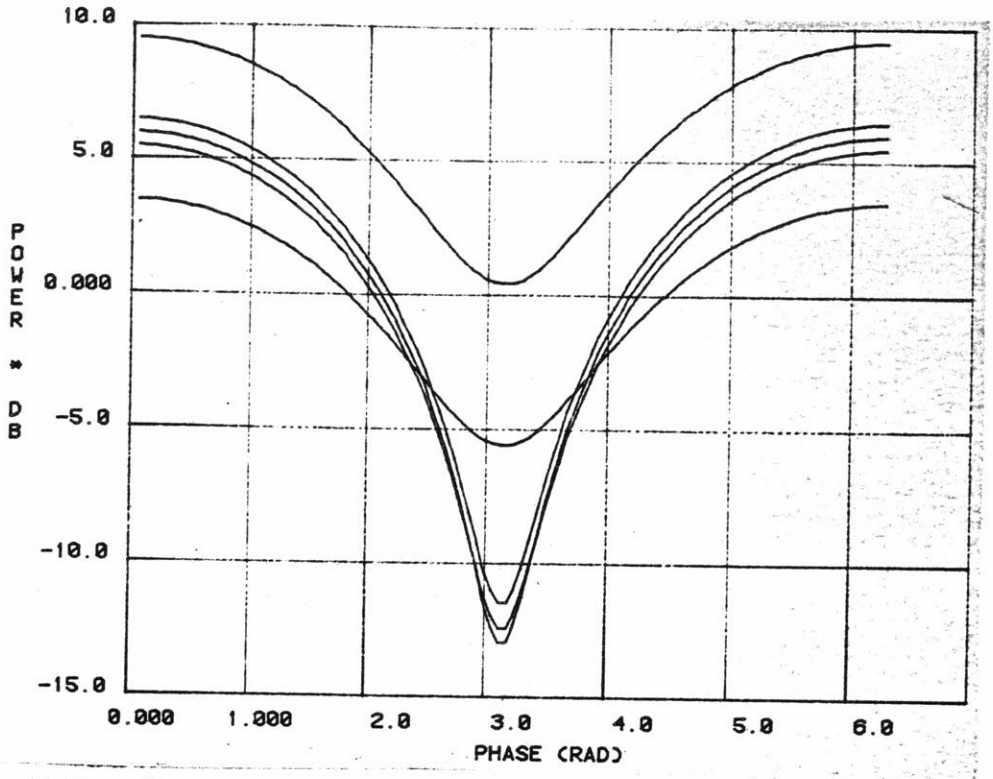


Figure 3-3. Power radiated by two point sources separated by $\lambda/20$. Vvn=1, $\psi_n$=0, argument $\psi_c$ varies from 0 to $2\pi$. From top to bottom along the vertical axis, the curves are for Vvc = 2, 1.12, 1, 0.89, 0.5.

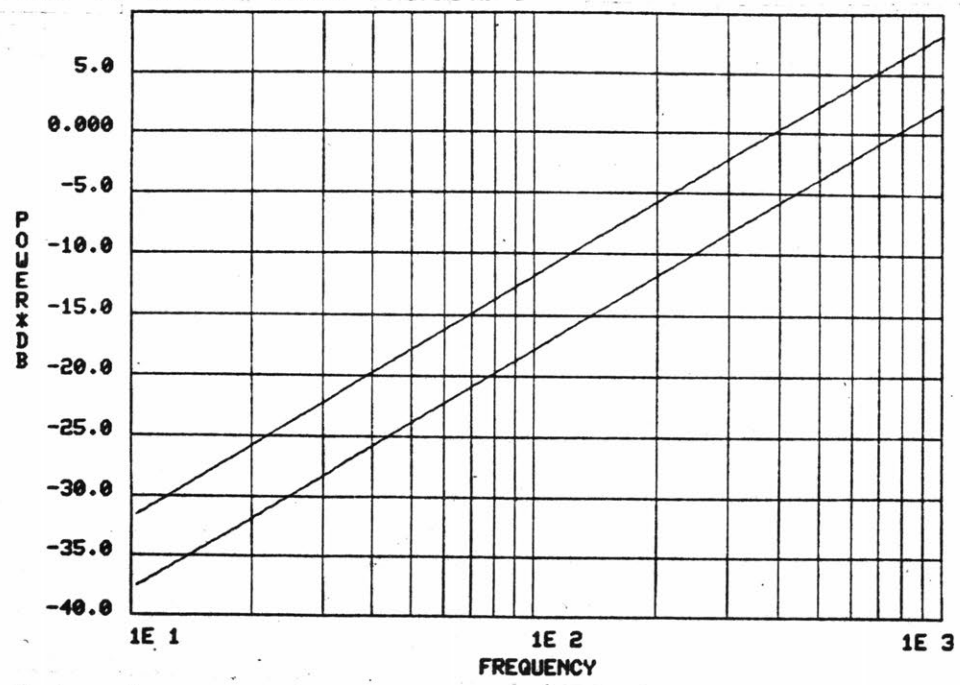


Figure 3-4. Power radiated by two point sources. Vvn=1, $\psi_n$=0, Vvc=1, $\psi_c=\pi$. Top curve: 0.2m source separation. Bottom curve: 0.1m source separation.

condition, that is, $\underline{V}_{vn} = -\underline{V}_{vc}$. For this dipole situation, a plot of power attenuation versus frequency is shown in figure 3-4 when the noise and attenuation source are located 0.1m apart. The programs used to generate these plots are shown in Appendix 4. Not surprisingly, at low frequencies, the attenuation is greatest, where the spacing of the sources is the smallest fraction of a wavelength. As this fraction becomes larger, less and less attenuation is observered. At frequencies near 500 Hz, the separation becomes significant compared to a wavelength, and the approximations used in deriving the power radiation equations are no longer valid. As a result, the results shown in the plot can not be regarded as reliable above 500 Hz. However, significant attenuation can not be expected when the sources are separated by a large fraction of a wavelength. In addition, the stability constraints imposed on the system will prevent the attenuating source from having significant output at these frequencies, and so the addition of the attenuating source will have little affect on power radiated at midband and high frequencies.

In general, acoustic sources are not point sources. One might expect, though, that by using reasonably sized loudspeakers as attenuating sources, each may be modeled accurately as a point source at frequencies where the attenuator functions. However, many noise sources can not be modeled accurately using point sources. But, any noise

source may be regarded as a collection of point sources, each having a different location, and complex volume velocity.

The total power radiated by M noise sources and one attenuating source is shown in equation 3-21 below.

$$P \propto Vvc^2 + \sum_{i=1}^{M} Vvn_i^2 + Vvc \cdot \sum_{i=1}^{M} Vvn_i \left( 2 - \frac{k^2 r_i^2}{2} \right) \cos \psi_i$$

$$+ \sum_{i=1}^{M} \sum_{\substack{J=1 \\ i \neq J}}^{M} Vvn_i \, Vvn_j \left(2 - \frac{k^2 r_{ij}^2}{2}\right) \cos(\psi_i - \psi_j) \qquad (3.21)$$

Power radiated by M noise sources at distance $r_i$, with magnitude $Vvn_i$ and phase $\psi_i$, and one attenuation source at the origin having magnitude Vvc and phase 0.

This expression is derived in Appendix 1, and follows steps similar to those in the derivation shown in this chapter. This expression turns out to be not particularly informative. However, one can note that as noise source to attenuating source spacings become smaller, the dipole situation causes increased power reduction. The goal again becomes making the attenuating source and each noise source as much like a dipole as possible. By doing so, the total power radiated can be reduced.

# Chapter 4

## SINGLE LOOP ATTENUATION OF SINGLE SOURCES

From the derivations of the previous chapter, the general form of the attenuation system is known. As was shown in that chapter, the attenuating source, for a single point noise source, should take the form of a point source, having volume velocity $\underline{V}vc(s) = -\underline{V}vn(s)$, and located as close as possible to the noise source. The next problem is to develop a system that generates this volume velocity.

It is expected that a closed loop system, as shown in figure 4-1, can fulfill the requirements. $\underline{V}vn(s)$ is the volume velocity of the noise source, and $\underline{V}vc(s)$ is that of the attenuating source. $\underline{H}(s)$ is the transfer function between the pressure at the microphone and the output device. The transfer function between the volume velocity of the noise source and sound pressure at the microphone is represented by $\underline{nfn}(s)$, the near field transfer function of the noise source. Similarly, $\underline{nfc}(s)$ represents the transfer function from the attenuating source volume velocity to the sound pressure at the microphone. The system is assumed to

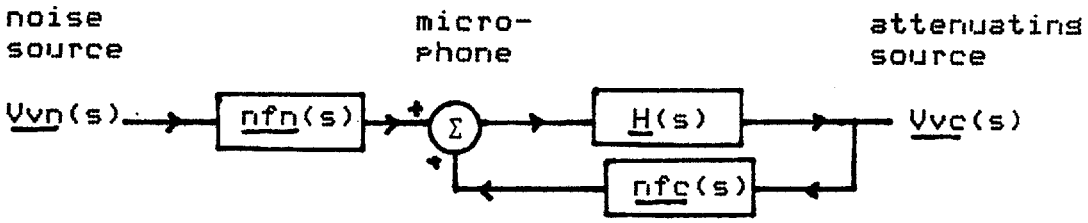


Figure 4-1. Closed loop attenuation system. $\underline{V}_{vn}(s)$ and $\underline{V}_{vc}(s)$ are the volume velocities of the noise source and the attenuating source, respectively. $\underline{nfn}(s)$ and $\underline{nfc}(s)$ are the near field transfer functions of the noise and attenuating sources, respectively. $\underline{H}(s)$ is the transfer function of the microphone, electronics, and speaker.

be linear and time invariant. The transfer function between $\underline{V}_{vc}(s)$ and $\underline{V}_{vn}(s)$ can be written

$$\underline{V}_{vc}(s) = \frac{\underline{H}(s)\ \underline{nfn}(s)}{1 - \underline{H}(s)\ \underline{nfc}(s)}\ \underline{V}_{vn}(s) \qquad (4.1)$$

When $\underline{nfn}(s) = \underline{nfc}(s)$, and when $|\underline{H}(s)\ \underline{nfc}(s)| >> 1$, then this equation reduces to $\underline{V}_{vc}(s) = -\underline{V}_{vn}(s)$, which is precisely the transfer function desired. So, in order to obtain the proper attenuator action, $\underline{H}(s)$, and thus the open loop gain, of the system must be large, and the near field pressure transfer function must be the same for both the noise source and the attenuating source.

The practical restrictions on the near field transfer functions, $\underline{nfn}(s)$ and $\underline{nfc}(s)$, and on the system transfer function, $\underline{H}(s)$, must be determined to ensure that $\underline{V}_{vn}(s) = -\underline{V}_{vc}(s)$ in a practical system. Before investigating the requirements on $\underline{H}(s)$, the near field transfer functions

should be examined. The simplest case, a point noise source, implies a point attenuating source at an equal distance from the microphone, so that $\underline{nfn}(s) = \underline{nfc}(s)$. For frequencies of interest, it is possible to build a loudspeaker system which will act as a point source in both the near and far field. The speaker enclosure must be sealed, and all dimensions of the loudspeaker enclosure must be small compared to a wavelength at the highest frequency of interest. If, for example, the highest frequency of interest is 500 Hz, the wavelength is 70cm, and all dimensions of the loudspeaker must be small compared to 70cm.

In order to examine further the near field properties of a loudspeaker, some pressure measurements were made of a loudspeaker in an anechoic chamber. A loudspeaker, consisting of a 6 inch diameter high displacement woofer enclosed in a sealed box having approximate dimensions 20 x 23 x 30cm, was excited by swept sine waves. At various distances from the speaker, a microphone measured the on-axis sound pressure. The amplitude and phase of this pressure compared to the loudspeaker excitation is shown in figure 4-2. The top plot shows the magnitude of the loudspeaker to microphone transfer function for microphone to speaker distances of 5cm and 100cm. The bottom plot shows the phase function for both distances. The only significant difference at low frequencies between the two curves in each plot is the added frequency dependent phase term due to the transit time

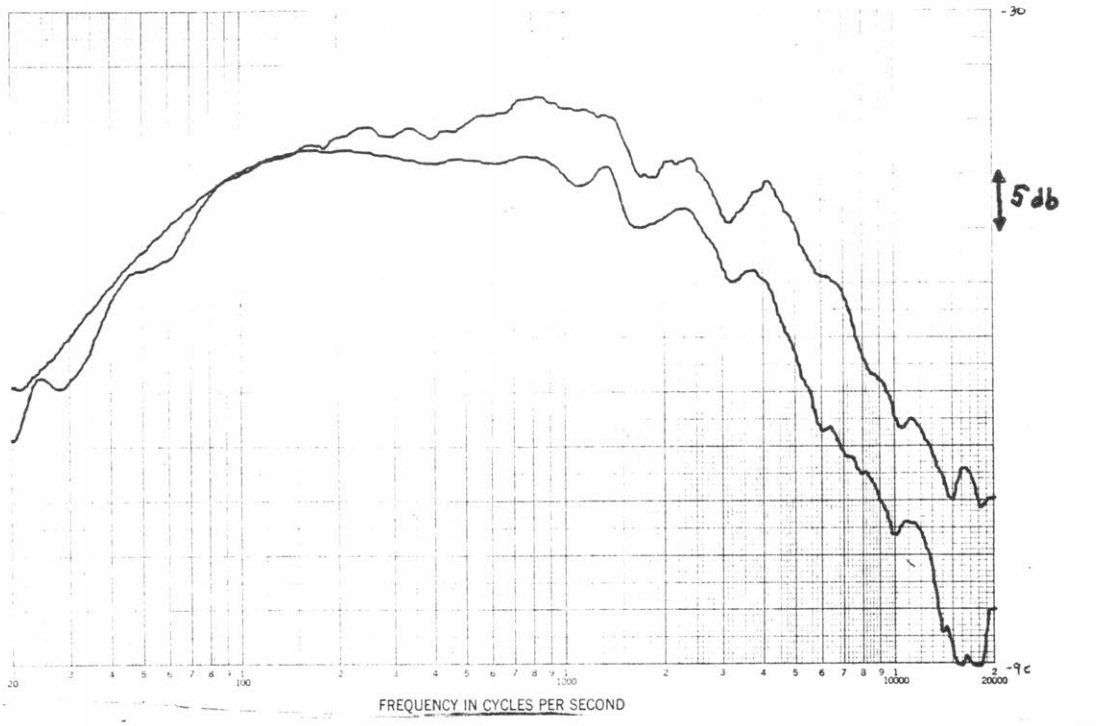


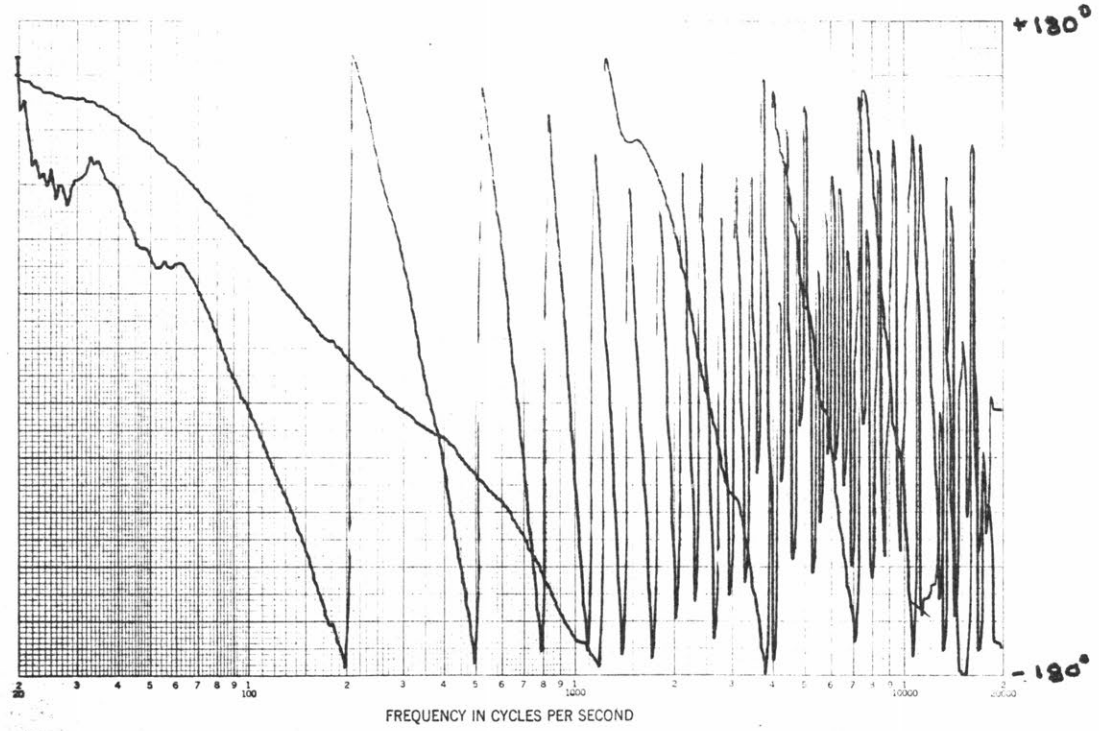


Fisure 4-2. Masnitude and phase measurements of the experimental speaker in an anechoic chamber. Top plot: magnitude curves. Top curve: 100cm microphone to speaker spacing. Bottom curve: 5cm spacing, scale shifted by 30 db. Bottom plot: phase curves. Top curve: 5cm spacing. Bottom curve: 100cm spacing.

delay. These plots indicate that like a point source, the loudspeaker has a far field transfer function which is the same as its near field transfer function at low frequencies, where dimensions are small compared to a wavelength.

The noise source, as discussed earlier, may not be particularly well modeled as a point source. However, any noise source may be considered as a collection of point sources, in which case, the effect of the attenuator is to try to make the collection of nearby point sources and itself into a dipole. Significant attenuation can be attained even when the noise source is not a point source, as is shown theoretically in Appendix 2, and experimentally below.

Assuming, for the moment, that the noise source is a point source, then in order to make nfn(s) and nfc(s) identical, the distance from the microphone to each of the sources must be the same, as shown in Chapter 3. This condition will ensure that the two transfer functions are equal.

The first condition, that nfn(s) = nfc(s), has been satisfied. The next, that H(s) be large, must be examined. H(s) is the transfer function from the pressure at the microphone position to the volume velocity of the attenuating loudspeaker. It includes the frequency response of the microphone, the electronics, and the loudspeaker.

For the system under consideration, which is open loop stable, and whose magnitude curve passes through unity only

once, or remains less than unity, each time the phase curve passes through 180 degrees, the closed loop system is stable if the loop gain is less than unity at the frequencies where the phase passes through 180 degrees. Both the microphone and the loudspeaker contribute to the magnitude and phase of the system, so models of these two devices must be obtained before the electronics can be designed.

The speaker used for the attenuator source was the same one as used in the anechoic near field measurements discussed above. As described in Appendix 3, measurements of the loudspeaker were made, and an electrical model was constructed. In order to verify the accuracy of the model, the measured driving point impedance was compared to that predicted by the model. The computer circuit analysis program, TWEAK, developed at Bose Corporation, was used to generate an impedance curve for this speaker model. This computed impedance curve matches quite well the measured impedance curve of the actual speaker, as shown in figures 4-3 and 4-4. The primary region of disagreement is in the high frequency end, due to the skin effect in the speaker pole piece. Since this effect occurs only at frequencies above those of interest, it was left out of the model.

The analysis program was also used to generate a gain and phase curve for the transfer function of the loudspeaker. The input parameter is the voltage driving the speaker, and the output is the far field pressure, which for frequencies

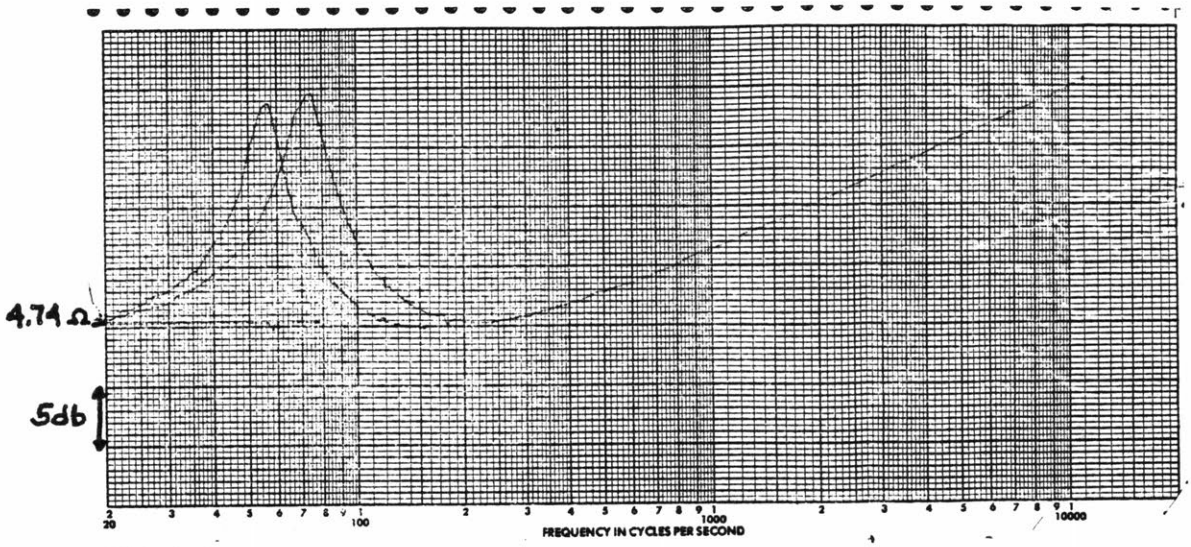


Figure 4-3. Measured impedance curve of experimental loudspeaker. Curve with higher frequency peak is the correct curve. Second curve was used for calculating model parameters as discussed in Appendix 3.

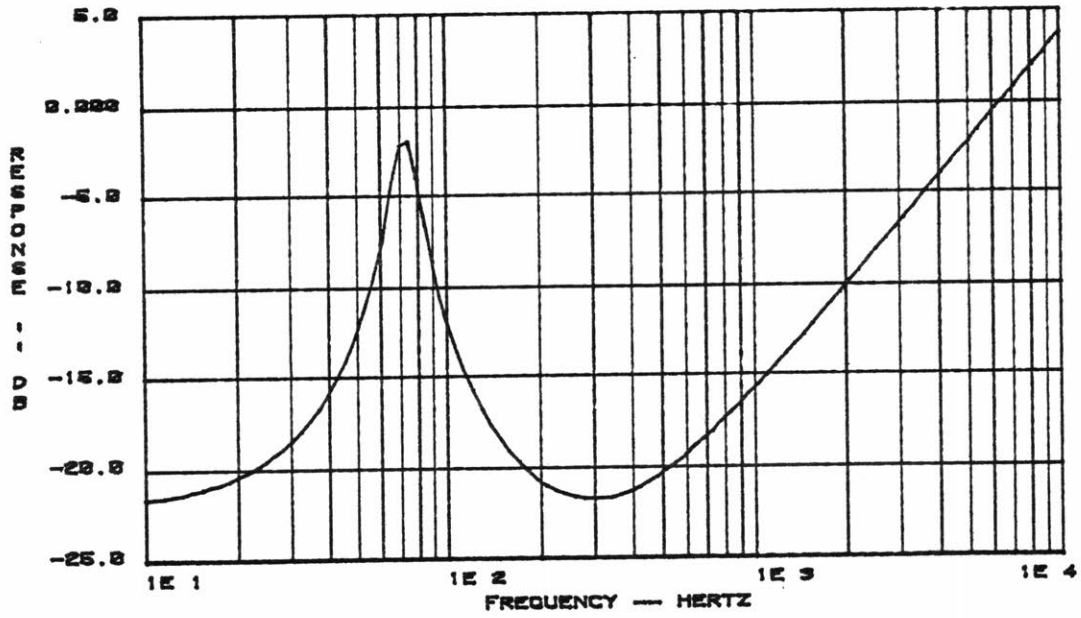


Figure 4-4. Calculated impedance curve for experimental loudspeaker.

of interest, is proportional to the near field pressure, as verified in the experiment used to generate figure 4-2. The plots are shown in figure 4-5. Listings of the computer files used as input to the circuit analysis program are shown in Appendix 5. The zero db level of the magnitude plot is

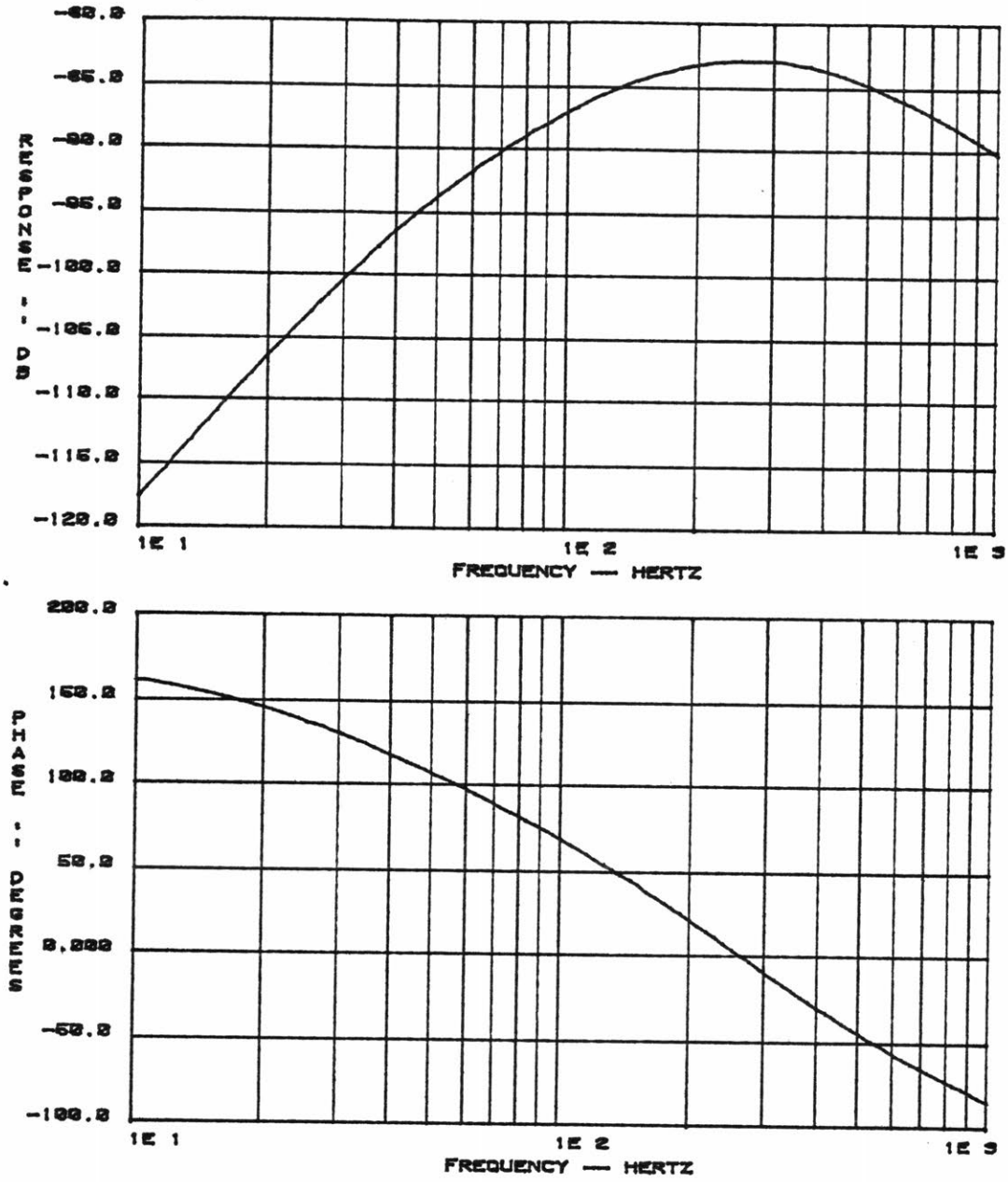


Figure 4-5. Calculated magnitude and phase curves for experimental speaker. Voltage applied to the speaker is the input, and far field pressure is the output.

relative and does not refer to any particular level of interest.

The microphone used in the experiments was a small (7 x 7 x 5mm) electret microphone with an integrated preamplifier,

Knowles Electronics model CA-1832. The frequency response of the actual microphone used was measured to verify its performance. The low frequency cutoff of the microphone was found to be 25 Hz by another investigator in the lab, and was confirmed using open loop gain and phase measurements of the completed system. A zero at the origin, and a real pole at 25 Hz was added to the loudspeaker model to include the effects of the microphone in the system. The computer calculated magnitude and phase response of these two elements is shown in figure 4-6.

The only remaining non-electronic element in the system was the air separating the microphone and loudspeaker. The gain of this element is a constant, depending on the separation, but the phase is a strong function of frequency, due to the time delay. In order to model this delay, an all-pass filter was added to the computer model which, over the frequencies of interest, approximates the phase response of the delay corresponding to 5cm of air. This distance was selected because it was thought to be representative of the typical distance that might be used in a practical system. The resulting calculated gain and phase curves are shown in figure 4-7. The all-pass filter adds 180 degrees of phase to the system that does not exist in the air path. Thus, the phase angle marked zero degrees actually represents a phase angle of 180 degrees. So, for stability, the electronics must have a gain of less than one at the frequencies where

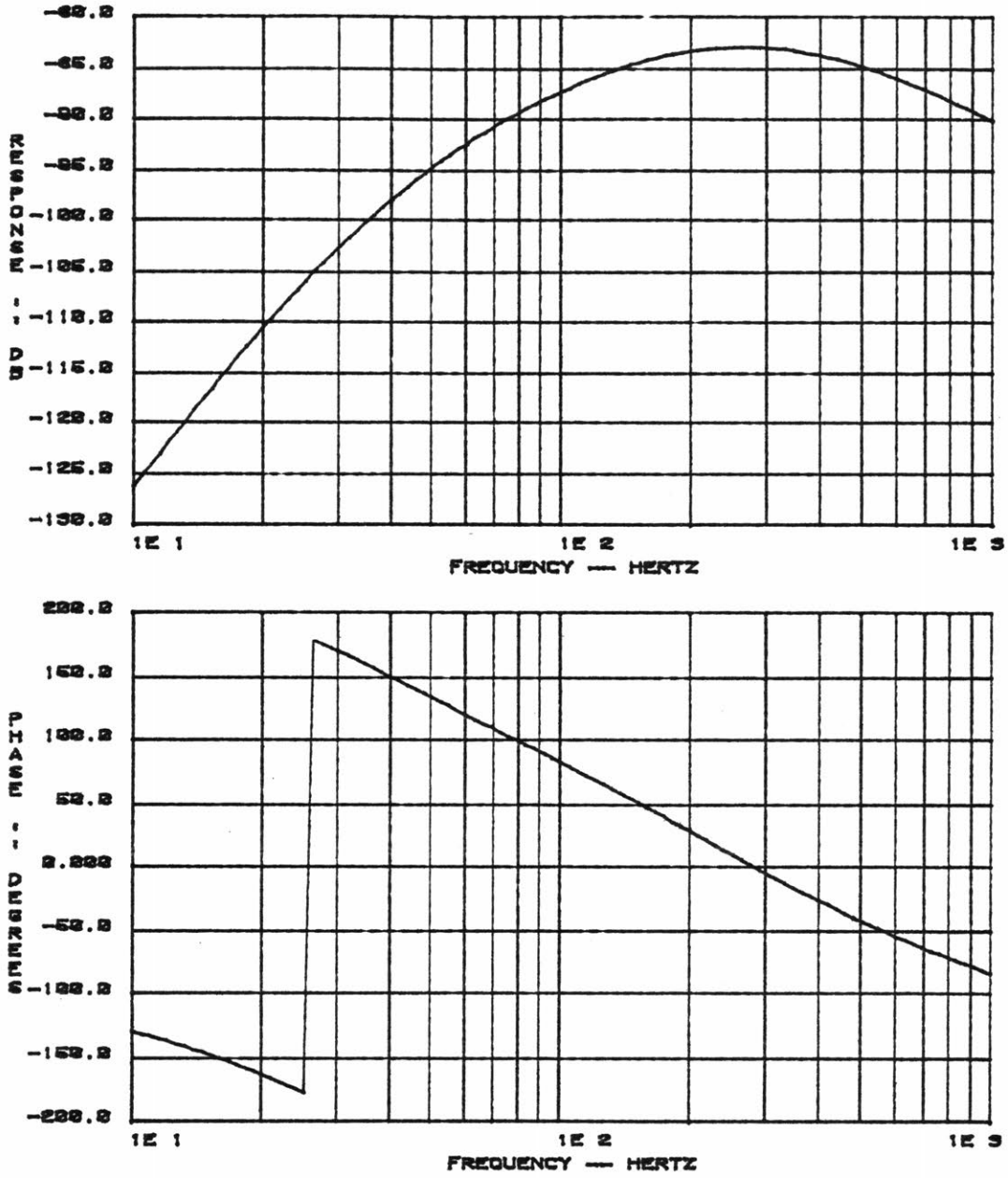


Figure 4-6. Calculated magnitude and phase curves for speaker and microphone.

the phase curve crosses the zero degree line on these computer plots. This error continues for the remainder of the computer generated plots shown in this chapter.

In order to verify the accuracy of the computer model, open loop gain and phase measurements were made on the actual

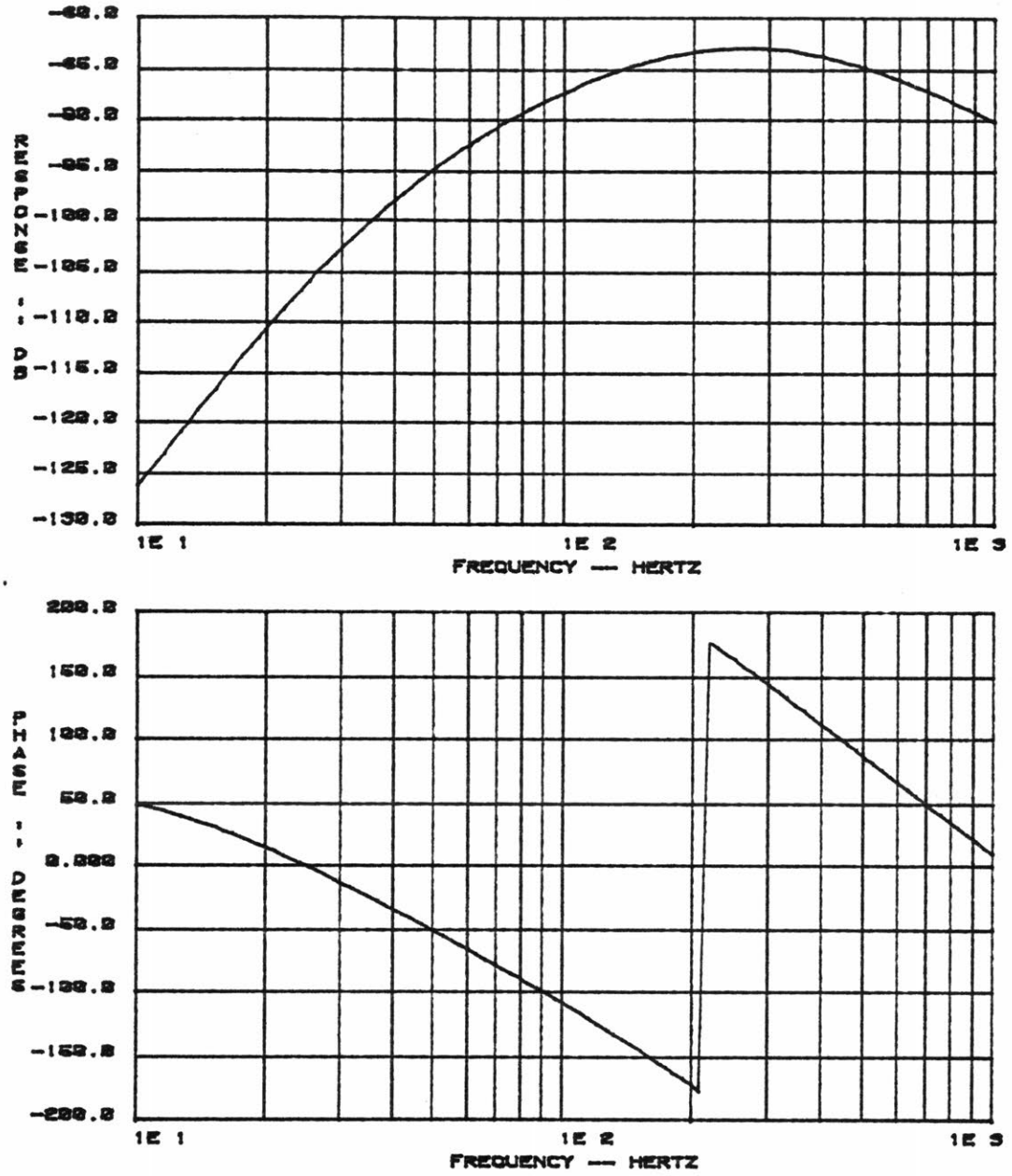


Figure 4-7. Calculated magnitude and phase curves for speaker, microphone, and a 5cm air path. Note that phase curve is incorrect by 180 degrees as explained in the text.

system. The results of those measurements are shown in figure 4-8, and seem to match the computer model well, particularly the two important parameters of crossover

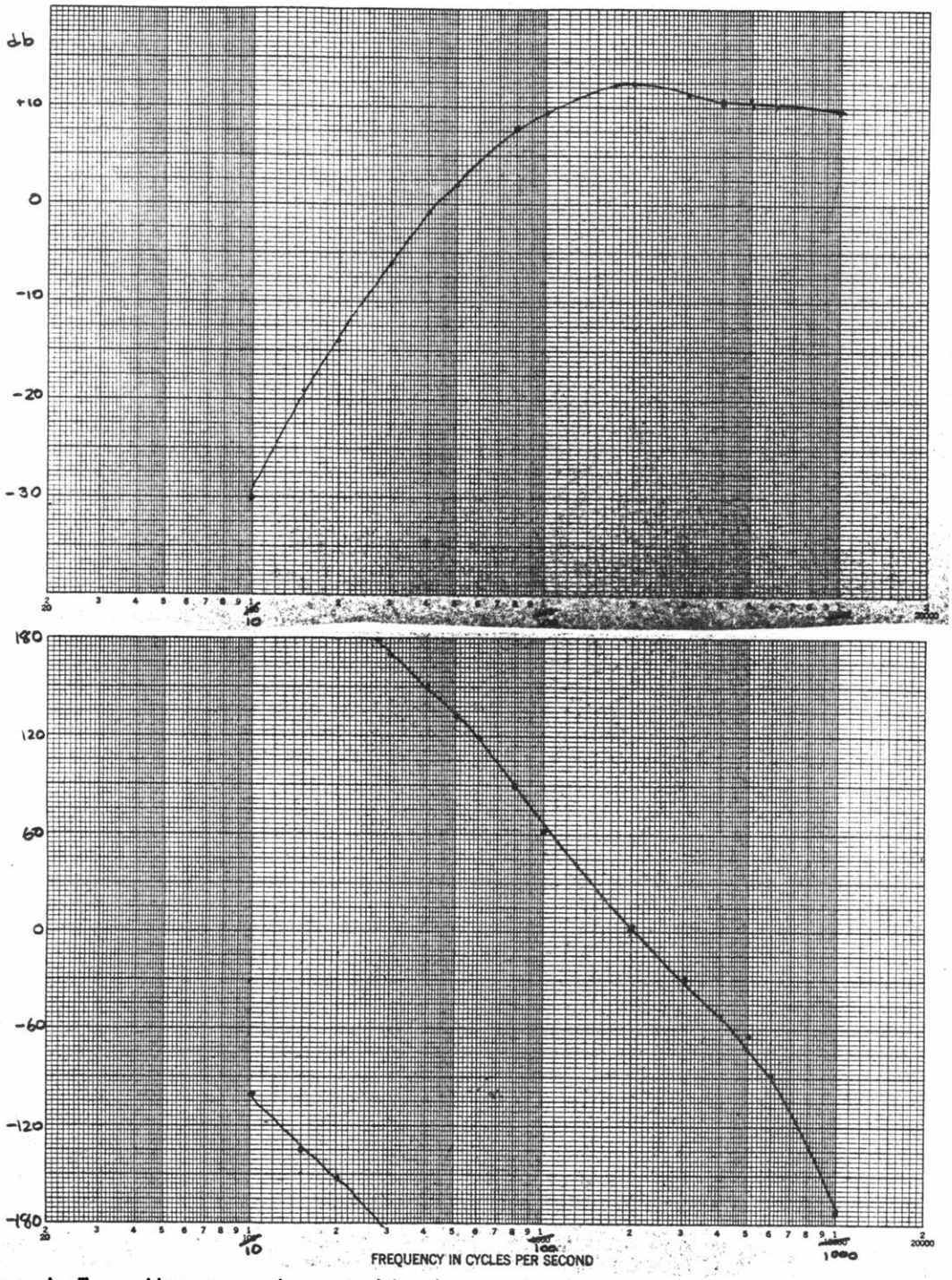


Figure 4-8. Measured magnitude and phase curves for speaker, microphone, and 5cm air path.

frequency and maximum open loop gain.

The goal is to make the open loop gain as large as possible over as wide a frequency range as possible while keeping the gain less than one where the phase crosses

through 180 degrees. This goal can be achieved through the use of compensation in the electronics path. After some calculation and a series of trials, it was found that a single real pole at 25 Hz, and a double lead/lag network, providing two real poles at 80 Hz, two at 3000 Hz, and two real zeros at 160 Hz and two at 1500 Hz, seemed to provide as much open loop gain over as wide a frequency as any of the other compensation schemes modeled on the computer. The open loop magnitude and phase plots as calculated by the computer are shown in figure 4-9. This compensation gives a maximum open loop gain which is 16 db above the gain at the crossover frequency, with crossover occuring at 15 and 500 Hz.

One disappointment is the fact that the maximum open loop gain is not as high as one might like. This open loop gain gives a measure of how much pressure reduction at the microphone can be expected, which in turn, indicates the amount of power reduction that can be achieved. This maximum open loop gain is limited by the fact that the system gain must fall off asymptotically no faster than second order, that is, 12db per octave, at the crossover frequencies, in order for the system to be stable. So, in order to increase the maximum open loop gain while keeping a reasonable amount of gain throughout the region between crossover frequencies, the crossover frequencies should be separated as much as possible. By putting the low end crossover frequency as low as possible and the high end crossover frequency as high as

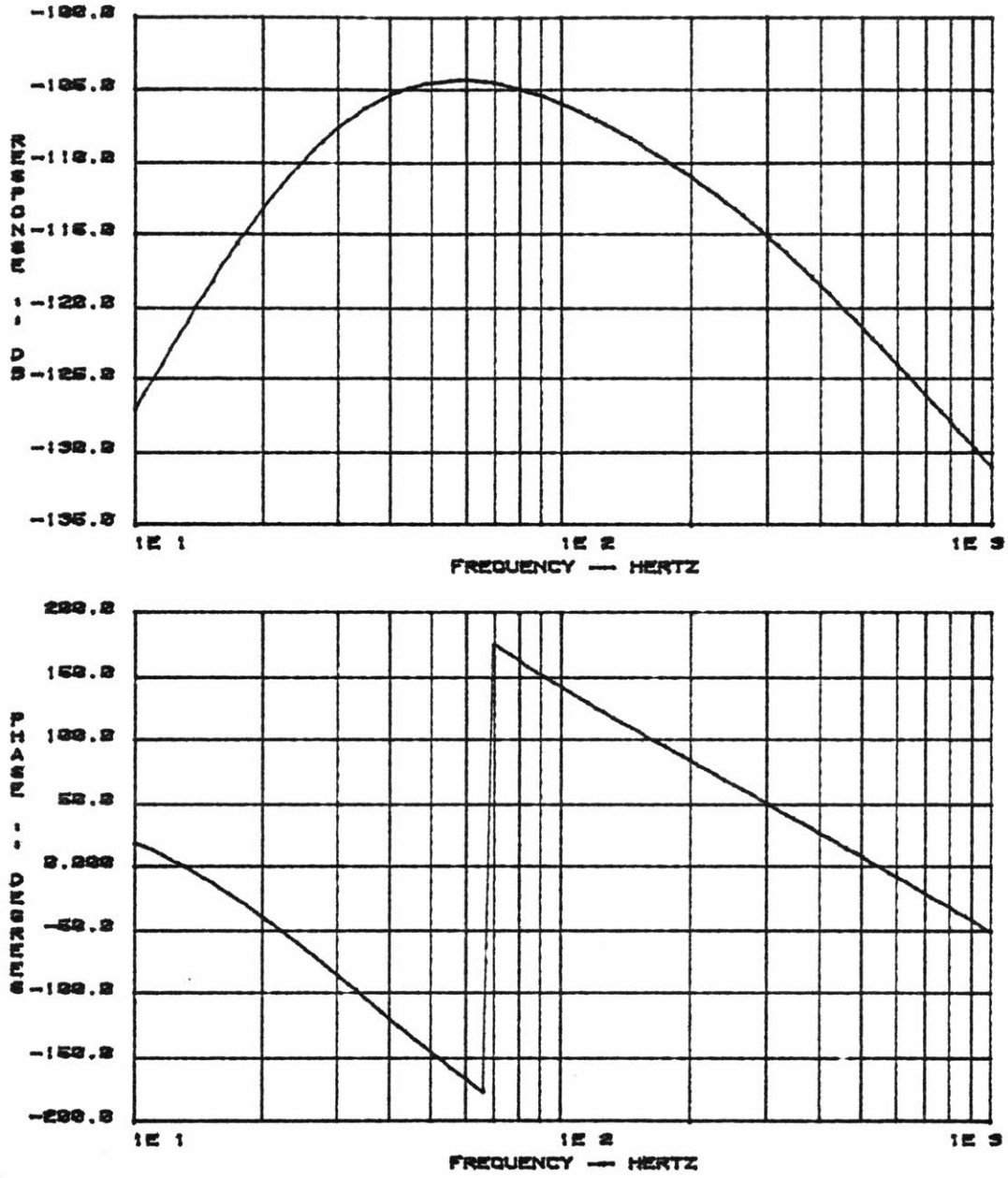


Fisure 4-9. Calculated masnitude and phase curves for the complete open loop system.

possible, a hisher maximum open loop sain can be achieved, and sisnificant sain, and thus sisnificant attenuation, can occur over a wider band of frequencies.

However, several physical constraints prevent this

improvement. On the high end, the crossover frequency can not be extended too far, since the phase shift due to the time delay in air becomes significant and causes instability. 500 Hz is a reasonable upper limit to the high end crossover frequency. (At 500 Hz, 0.1 meters corresponds to a phase shift of 50 degrees, already a significant fraction of the maximum allowable 180 degrees.) At the low end, however, it might seem that there would be no limitation to how low the crossover frequency could be set. Unfortunately, this thought is incorrect. The system attempts to set the pressure at the microphone to be zero. Below loudspeaker resonance, (which is approximately 80 Hz for the speaker used in these experiments) the speaker displacement must quadruple each time the frequency is cut in half for constant pressure output. So for each octave the cutoff frequency is decreased, the speaker must be able to move four times as far. At some point, the speaker becomes nonlinear, and additional displacement can not be obtained. Thus, a limit on the low frequency cutoff is imposed by the practical constraints of the loudspeaker. This problem is exacerbated by the high level of very low frequency noise present in most rooms, which gets picked up by the microphone and fed to the speaker. Thus, even in the absence of any noise sources to attenuate, the speaker may be traveling beyond its linear range.

Due to the large amount of ambient noise encountered

between 5 and 10 Hz, the low frequency cutoff frequency had to be held above 10 Hz for the speaker used in these experiments in order to avoid saturating the speaker displacement in normal operation. The low frequency cutoff frequency might be improved by using a larger loudspeaker enclosed in a larger box. The larger loudspeaker would not have to have as long a linear travel in order to obtain the same volume velocity, and since its resonant frequency would be lower, the problem of extending its response by increasing displacement at decreasing frequencies would be less severe. However, as the speaker system becomes larger, the attenuating source looks less and less like a point source, which violates previously stated assumptions. For this reason, the smaller, six inch speaker was used.

Another solution to the speaker displacement problem is the use of a port in the loudspeaker box. Such a port can greatly decrease loudspeaker displacement at the frequency of the port. However, such a port would complicate the design of the servo system, since below the port resonance, the port radiates, adding an additional source which must be taken into account in the servo analysis. Also, the port introduces an additional 12 db per octave rolloff in pressure response at low frequencies. Again, this alternative was not used in contrast to the simplicity of a sealed enclosure, which helps to limit extreme low frequency excursion and decreases the possibility of speaker damage due to excessive

displacement.

When the loop is closed, the computer model predicts a decrease in pressure at the microphone as shown in figure 4-10. If point noise and attenuating sources are assumed, the computer model predicts a global decrease in power as shown in figure 4-11. Again, due to the approximations used in deriving an expression for power radiated, the power plot is not accurate above approximately 500 Hz.

Over the range of frequencies from 20 to 300 Hz, according to the model, the power radiated by the noise source is decreased significantly by the addition of the attenuating system. This attenuation is maximum at 80 Hz, having a value of 21 db. At the low and high end of the operating range of the attenuating loop, the power is actually increased, due to the peaking in the closed loop response of the servo as the open loop phase passes through 180 degrees. At low frequencies, this increase can be made to occur well below audible frequencies, especially if the operating range of the system is extended as described above. At the high end, the increase is at a sufficiently high frequency that it could be attenuated passively. Thus, an increase in power radiated at these frequencies need not necessarily be a problem.

In the laboratory, the desired electronic compensator was constructed, as shown in Appendix 6. The attenuating system was set up, and its ability to reduce noise was

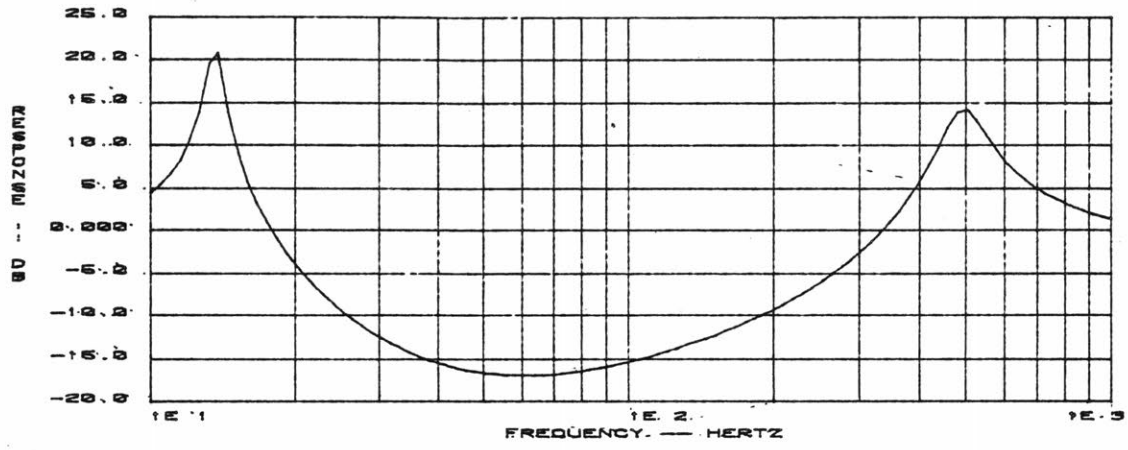


Figure 4-10. Calculated pressure reduction at the microphone in complete closed loop system.

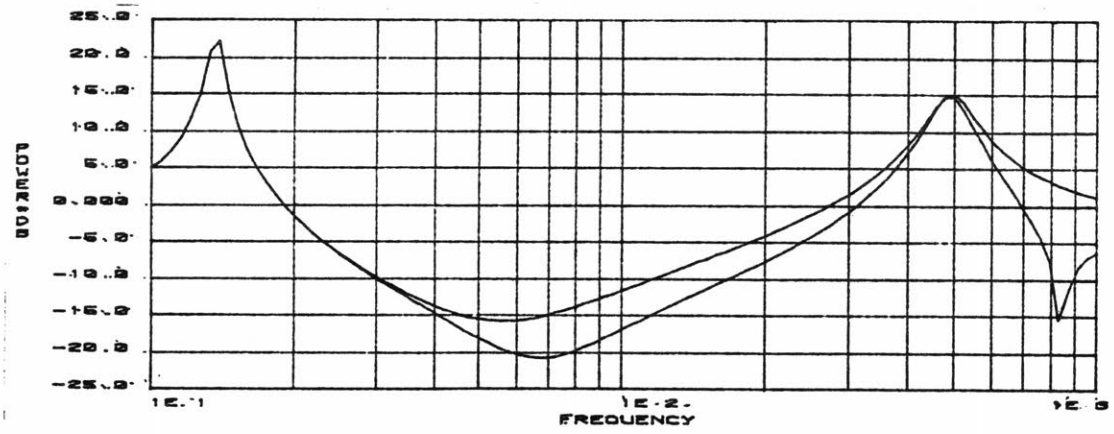


Figure 4-11. Calculated global power reduction due to complete closed loop system, with the microphone spaced 5cm from both sources, assuming point sources. Top curve: 0.2m separation between sources. Bottom curve: 0.1m separation.

measured. In order to get an idea of the performance of the system in a reasonable room, as opposed to an anechoic chamber, the system was set up in a room with the floor plan shown in figure 4-12.

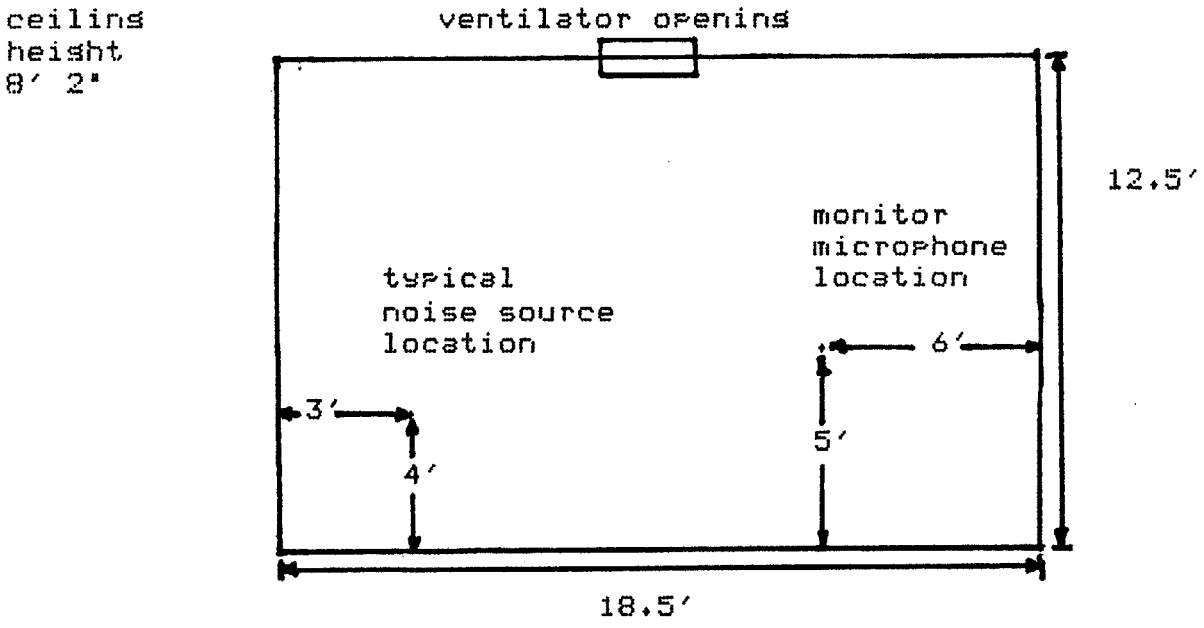


Figure 4-12. Floor plan of room in which attenuation experiments were conducted.

The room had been treated to reduce sound transmission from the outside of the room and to optimize its interior for these sorts of reverberant field sound measurements. The noise source was excited with wide band pink noise. The attenuating system was located near-by, with approximately a 5cm spacing between the microphone and both the noise and attenuating sources. A monitor microphone measured the

reverberant field sound pressure, which is dependent on the power radiated by acoustic sources into the room. Thus, the monitor microphone gave a measure of the power radiated by the sources. The microphone signal was filtered by a swept tenth-octave filter, and the output of the filter was plotted on a graphic level recorder.

The amount of attenuation the system provided is shown in the next four figures for various noise sources.

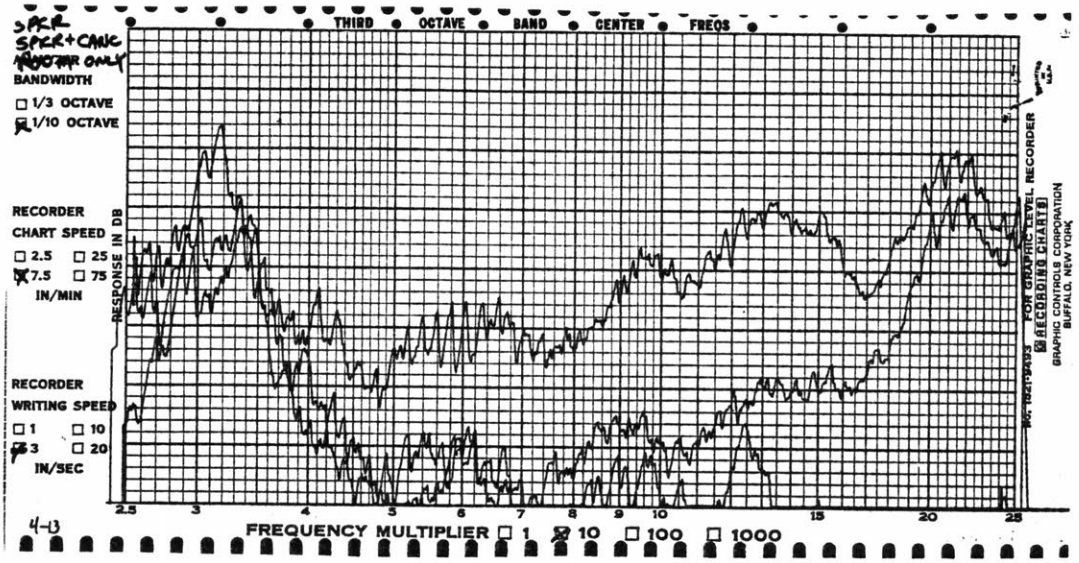


Figure 4-13. Measured reverberant field pressure for experimental speaker noise source. Top curve: noise source operating alone. Middle curve: noise source and attenuation system operating. Bottom curve: room and instrumentation noise, no sources operating in room.

In figure 4-13, the noise source was a loudspeaker identical to the one used as the attenuating source. The plot of reverberant field pressure shows a maximum reduction of 16 db occurring at 100 Hz. If this attenuation is compared to that calculated for point sources shown in figure 3-4, one sees that the attenuation provided by this system is about two db

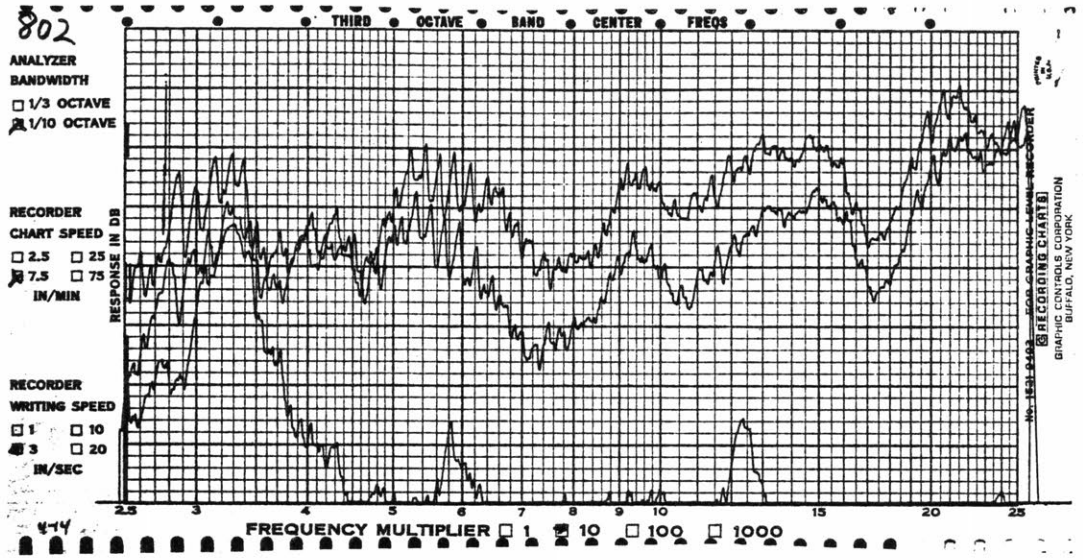


Figure 4-14. Measured reverberant field pressure for Bose 802 speaker noise source. Top curve: noise source operating alone. Middle curve: noise source and attenuating system operating. Bottom curve: no sources operating.

away from the theoretical maximum. At frequencies below 80 Hz, the sound level of the attenuator and noise sources was close to that of the room with no sources operating. Thus, the additional attenuation predicted by the computer model at these frequencies may have been hidden by the room noise.

For figure 4-14, the noise source was a Bose model 802 loudspeaker, a speaker measuring approximately 50 x 25 x 30cm, containing eight full range four and one half inch diameter drivers on one surface. The attenuating source was located opposite this face. Although the measured attenuation is not as great as the first experiment, significant attenuation was realized over the band from 40 to 250 Hz, with a maximum of 8 db at 70 Hz.

The bottom trace in these two plots is the sound level

measured by the monitor microphone with both the noise source and the attenuating source turned off. There is significant energy at 30 Hz, and at 60 Hz and its multiples. It is likely that a large portion of the 60 Hz energy is due to power line hum pickup in the instrumentation electronics, but a lot of the 30 and 60 Hz energy was introduced into the room by an open ventilation duct. Since the noise was troublesome while making other measurements, an attempt was made to quiet the duct using the attenuator system.

The duct opened into the room through the wall, approximately 1.5m from the floor, and had dimensions of roughly 45 x 30cm. The attenuating loudspeaker was placed directly below it, pointing up into the air flow. The microphone was positioned halfway between the speaker and the center of the duct, and shielded from the direct flow of air out of the duct by a piece of closed cell foam, to prevent wind noise from overloading the electronics. The reverberant field pressure measurements with and without the noise attenuator operating are shown in figure 4-15. The plots show that significant noise attenuation was achieved, with a maximum attenuation of 15 db at 50 Hz.

Finally, in what was thought to be a most difficult test of the attenuator's abilities, a small motor driven air compressor was brought into the room. The compressor consisted of a one third horsepower motor driving a two cylinder air compressor putting out air directly into the

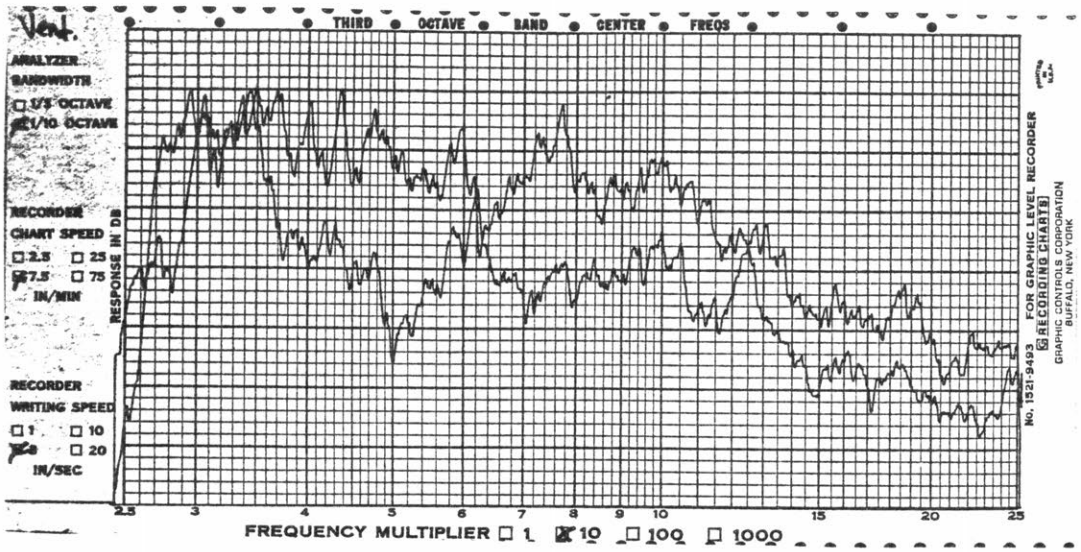


Figure 4-15. Measured reverberant field pressure for ventilator noise source. Top curve: ventilator alone. Bottom curve: ventilator and attenuator system operating.

room through a one eighth inch diameter orifice. The compressor was approximately 40cm long and 20cm in diameter. The attenuating speaker was placed close to the cylinder head of one of the cylinders. The plot of reverberant field pressure with and without the attenuator system in operation is shown in figure 4-16. Attenuation of 5 db over a wide band was achieved.

There are several possible explanations for the disparity between the predicted amount of noise reduction and that actually obtained. Firstly, for some types of noise sources, such as a dipole, significant attenuation can not be obtained, as shown in Appendix 2. The air compressor, having two opposed cylinders, probably had a significant dipole component. Thus, the noise reduction observed was

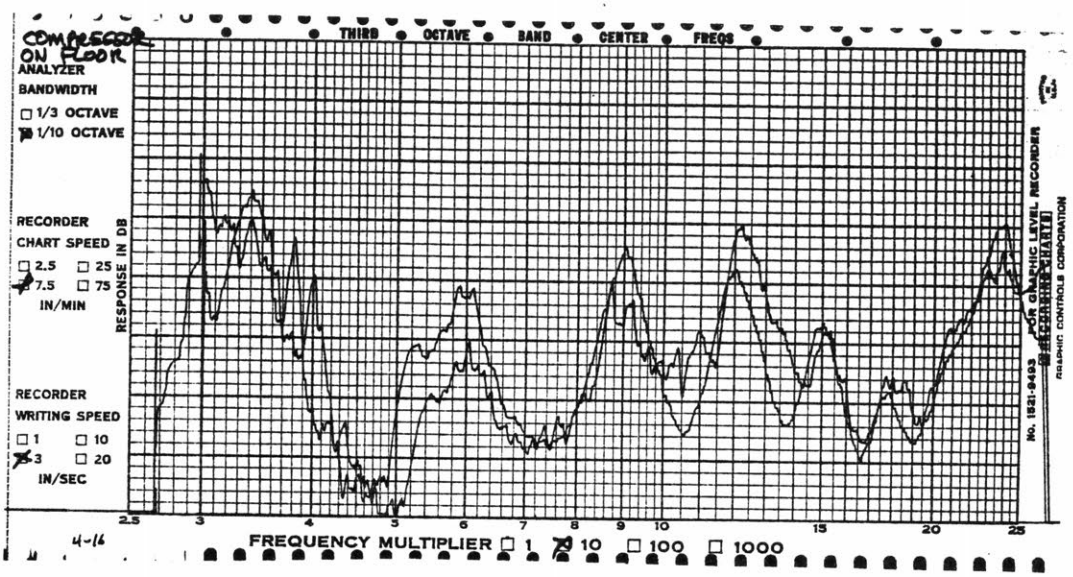


Figure 4-16. Measured reverberant field pressure for compressor noise source. Top curve: compressor alone. Bottom curve: compressor and attenuator system operating.

considerably less than that predicted assuming point sources. In the case of the Bose 802 loudspeaker, which at frequencies of interest can be modeled as a number of in-phase point sources, the attenuator system is most effective for those point sources spaced the same distance from the microphone as the attenuator speaker. For an extended noise source, such as the 802, having sources with significant volume velocities at a variety of distances from the microphone, only those sources spaced the correct distance from the microphone would be maximally attenuated, while the others would be attenuated to a lesser degree. Thus, the observed noise reduction with this noise source is less than that predicted.

These experiments indicate that the noise attenuating system constructed in the lab performed at levels close to

the theoretical limits calculated earlier, when used under ideal situations. But, even under nonideal situtations, much more like those likely to be encountered in practice, the attenuator performed surprisingly well, reducing the noise generated by several typical noise sources.

# Chapter 5

# MULTIPLE LOOP ATTENUATION OF NOISE SOURCES

The work of the previous chapters has shown that it is possible to reduce the acoustic power radiated by small sources. However, there exist many noise sources whose dimensions are not small compared to a wavelength. At 80 Hz, the frequency for which the single loop attenuator has the best performance, a wavelength is approximately 4 meters, so a noise source must have dimensions significantly smaller than this figure in order to obtain reasonable noise attenuation. This restriction severely limits the usefulness of the noise attenuating scheme. However, for large noise sources, it might be possible to use several attenuating loops, located around the noise source, to provide better attenuation than one loop alone could provide. Additionally, there is the possibility that there might be several discrete noise sources in a room, each having its own attenuating loop. In either case, a multiplicity of attenuating loops might provide better performance than one. However, multiple loops in close proximity could create stability difficulties.

The simplest case to consider is that of a single point noise source, and two point attenuating sources. A measure of the increase in attenuation that this system can provide compared to a single attenuating source system is needed. The equation developed in Appendix 1 can provide this measure.

$$P \propto Vvn^2 + Vvc_1^2 + Vvc_2^2 + Vvc_1\, Vvc_2 \left(2 - \frac{k^2 r_{12}^2}{2}\right) \cos(\psi_1 - \psi_2) + Vvn\, Vvc_1 \left(2 - \frac{k^2 r_1^2}{2}\right) \cos\psi_1 + Vvn\, Vvc_2 \left(2 - \frac{k^2 r_2^2}{2}\right) \cos\psi_2 \qquad (5.1)$$

The equation assumes a noise point source located at the origin, with volume velocity magnitude 1 and phase 0. One point attenuating source is located at $(r_1,0)$, with magnitude $Vvc_1$ and phase $\psi_1$. The other is located at $(r_2,\theta_2)$, with magnitude $Vvc_2$ and phase $\psi_2$. $r_{12}$ is the distance between attenuating source 1 and 2.

The power radiated can be minimized by setting $Vvc_1$ and $Vvc_2$ to 0.5, $\psi_1$ and $\psi_2$ to 180 degrees, and $r_{12} = 2\, r_1$. Under these conditions, the equation predicts a total radiated power of zero. In fact, the small amount of power actually radiated by the sources is hidden in the approximations used in deriving equation (5.1). If an additional term in both the sine and cosine expansions is retained, as shown in

Appendix 1, a more accurate measure of power is obtained. Under the geometric conditions used to generate figure 3-3, a dipole yields a 14 db power reduction, while a tripole provides 26 db.

The addition of the third source increases the order of the resulting multipole source. For three sources, it has just been shown above that a tripole minimizes power radiated. Using equations derived in Appendix 1, it can be shown for the four source case that a quadripole minimizes power radiated. It is expected that in an n-source case, a n-pole would minimize power radiated.

The increase in noise attenuation that is achieved in the three source case as the tripole condition is approached is shown in the plots of figure 5-1. In each of the plots, the volume velocity magnitudes and phases are as described above. In each, $r_1$ and $r_2$ are set to 0.1m, but $r_{12}$ varies from 0 to 0.2m. Zero db refers to the power radiated by a single point source with a volume velocity magnitude of 1. For the top plot, the second attenuating source is located at (0.1,0), so that it is superimposed upon the first attenuating source. This situation is identical to the single attenuating source situation described in the previous chapter. In the middle plot, the second attenuating source has been moved to (0.1, $\pi/2$). Some increase in attenuation is observed. In the bottom plot, the second attenuating source is located at (0.1, $\pi$). The radiated power should be

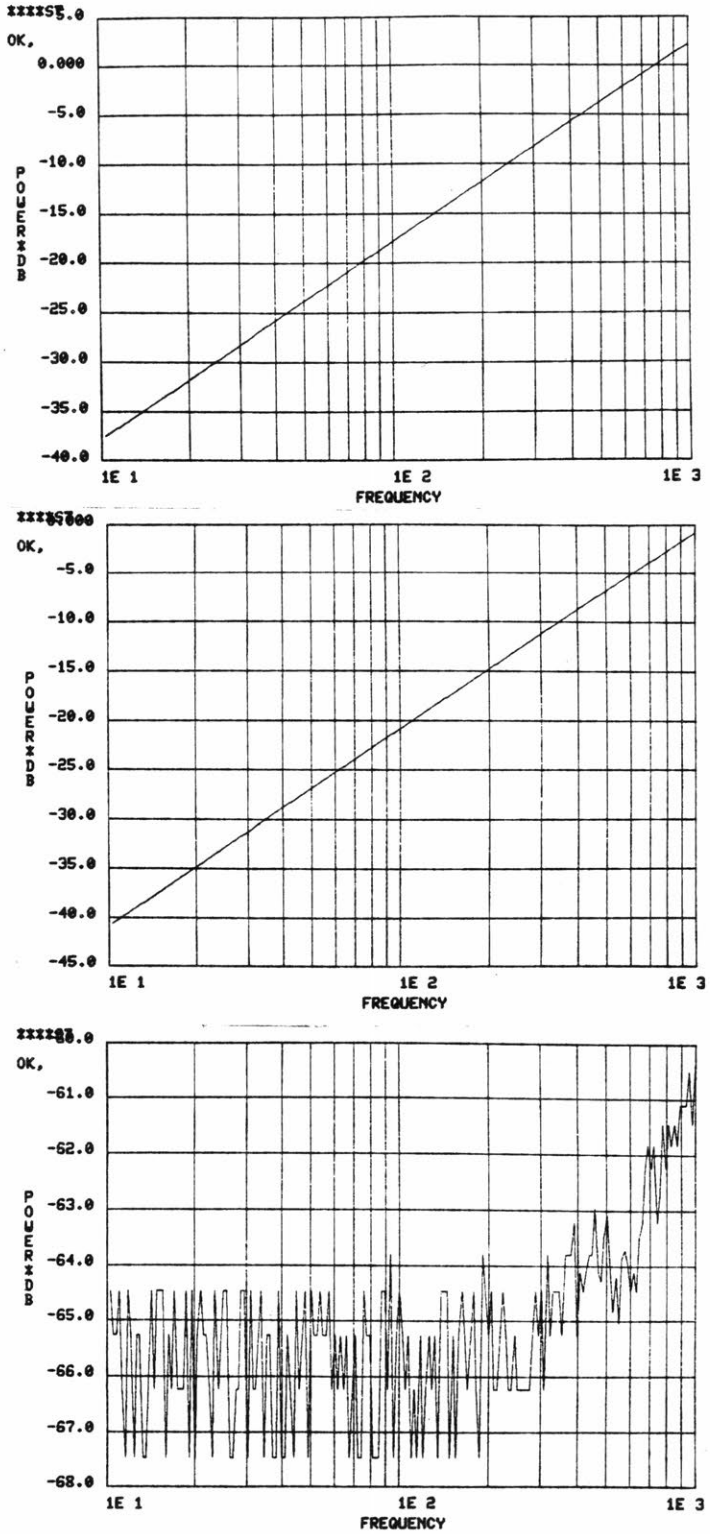


Figure 5-1. Power radiated by a single noise source and two attenuating point sources. $r_1 = r_2 = 0.1$m. Top plot: $r_{12} = 0$. Middle plot: $r_{12} = 0.1414$m. Bottom plot: $r_{12} = 0.2$m.

near zero, and the plot shows nothing other than the roundoff error of the computer.

Even with a point noise source, a second attenuating source can provide significant reduction in radiated power. The next problem is to determine the sort of system that is needed to produce the required volume velocities.

Again, a closed loop system is expected. The most general form of that system is shown in figure 5-2.

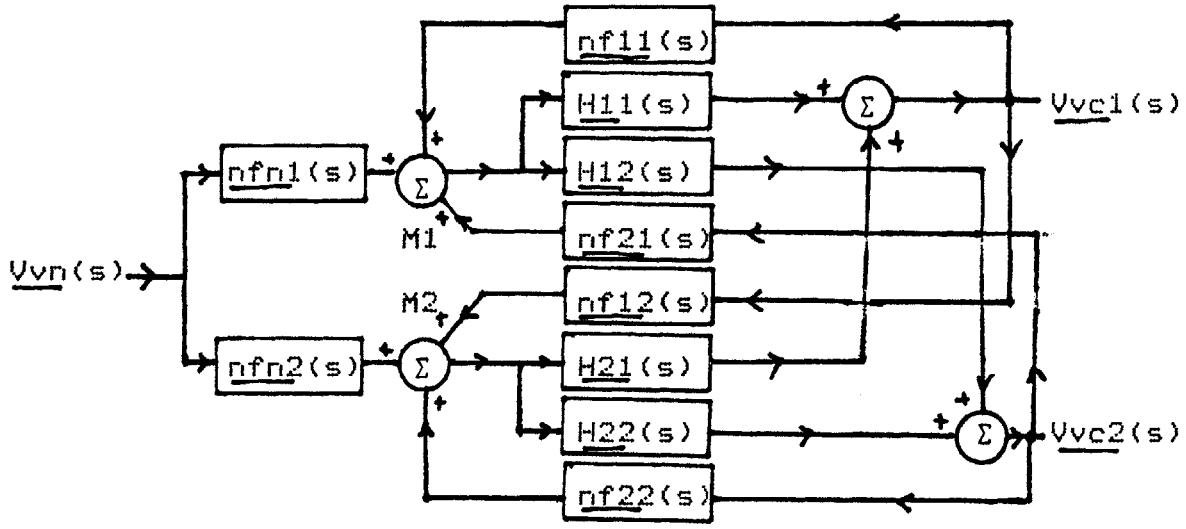


Figure 5-2. Two loop attenuating system diagram.

Refering to the figure, the transfer function from the volume velocity of the noise source to the pressure at each of the two microphones is nfn1(s) and nfn2(s), the near field sound pressure due to the noise source. Linking microphone i with attenuating source J is the transfer function Hij(s), which represents the frequency response of the microphone, system electronics, and loudspeaker volume velocity. From the

attenuating source i to microphone J is the transfer function nfij(s), the near field pressure of attenuating source i as measured at microphone J.

Equations can be written relating the attenuating source volume velocities with that of the noise source, but such equations do not provide any insight to the problem. In addition, there is a much more significant problem to be answered first, namely, the question of stability. The conditions that make this entire system stable need to be found.

Classical control theory, as used in the previous chapter, is unable to provide an answer to this question. Although in theory it is possible to write the equation governing the loop in the form $1 + F(s) = 0$ and use this equation to study stability, in practice, this job would be extremely difficult. It was hoped that modern control theory could provide some help. However, due to the time delays in the system, the problem is an infinite dimensional problem. In order to completely characterize the state of the system, the pressure must be known for an infinity of points between each of the sources and the microphones. Several recent papers and texts on this topic, such as those by Willsky (34), Wolovich and Ferreira (36), Wolovich (35), Davison and Wang (8, 9), and Kwakernack and Sivan (15), plus discussions with several workers in this field, lead to the realization that in order to solve the central problem, techniques still

being developed in the control theory field would have to be employed. Such techniques would require a significant investment in time and effort in order to explore this new field. Rather than turn this work into one primarily concerned with control theory, it was decided to see if some other method of answering the stability question could be found.

One method that could answer the question with a reasonable effort was the use of a time domain computer simulation of the system. It was decided to use this approach to try to gain some insight into the various aspects of the multiple loop attenuation problem. Although the computer simulation could help answer the question of stability, it was not intended that the model predict detailed behavior of the actual system. It was intended only to give a comparative indication of stability and performance as the various loop gains were changed. As a result, the model is an extremely simple one, with a number of approximations. Point noise and attenuating sources are assumed. Blocks which model the microphone, electronics, and loudspeaker of the actual system were simplified to the point where they contain only a single real pole and an adjustable gain. The model used is shown in figure 5-3, along with a listing of conditions assigned to the model. In order to implement this model on a computer, a second order predictor-corrector algorithm, as discussed in Chua and Lin (5),

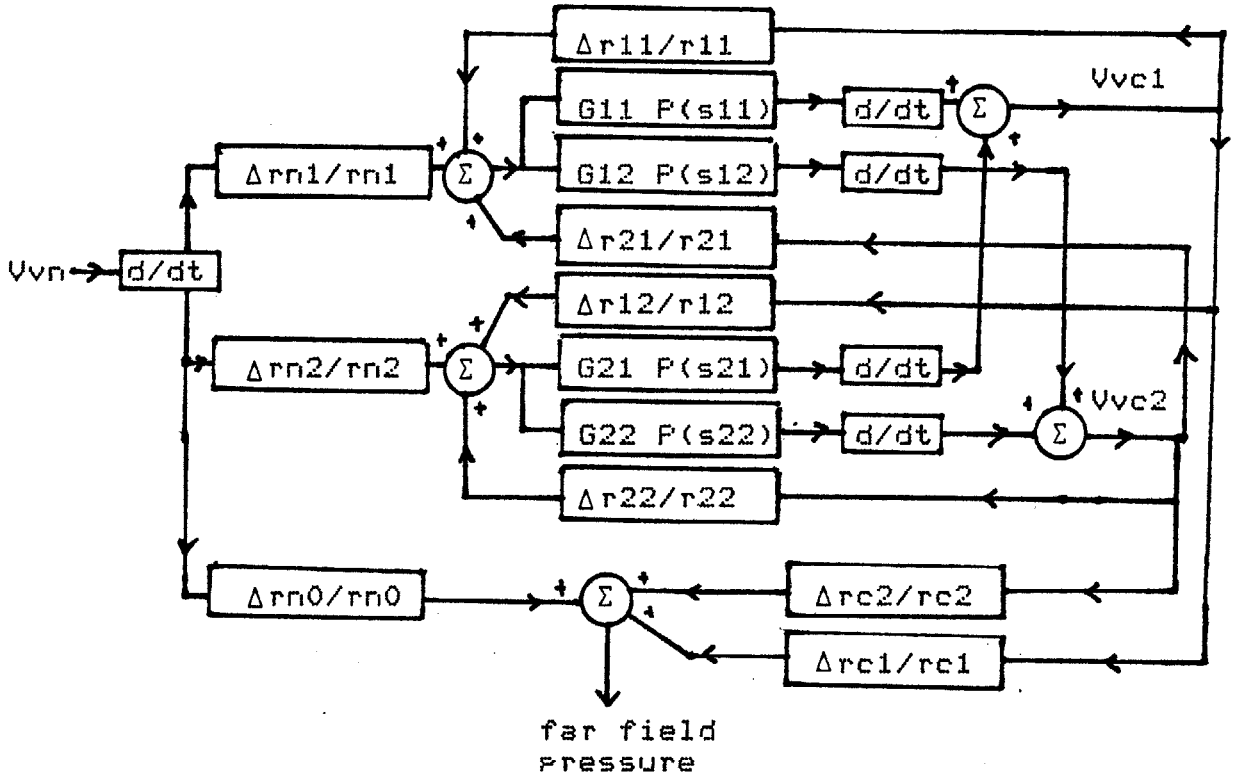


ΔrIJ/rIJ represents the delay and attenuation in path length rIJ. GIJ represents the gain, and P(sIJ) the pole, in feedforward path IJ.

| | | |
|---|---|---|
| r11 = 0.2m | rn1 = 0.2m | s11 = -600 rad/sec |
| r12 = 1.0 | rn2 = 1.0 | s12 = -600 |
| r21 = 1.0 | rn0 = 4.0 | s21 = -600 |
| r22 = 0.2 | rc1 = 4.1 | s22 = -600 |
| | rc2 = 4.2 | |

Figure 5-3. Two loop attenuating system computer model.

was used. A second order Adams-Bashforth predictor was used,

$$x_{n+1} = x_n + h\{\frac{3}{2} f(x_n, t_n) - \frac{1}{2} f(x_{n-1}, t_{n-1})\} \qquad (5.2)$$

and a second order Adams-Moulton corrector,

$$x_{n+1} = x_n + h\{\frac{1}{2} f(x_{n+1}, t_{n+1}) + \frac{1}{2} f(x_n, t_n)\} \qquad (5.3)$$

Since it was desired that each time delay in the system be represented by at least several time samples, the time between samples was set to 0.0001 seconds. This rate provided for 3 to 4 samples in the shortest delay.

The computer model was checked for correct operation by comparing its prediction to the known behavior of some simple systems, with satisfactory results. In order to examine system stability with the model, the system impulse response was found. With the system at rest, the noise source volume velocity was assigned to be an impulse function. The system output was the far field pressure. Using the bounded input, bounded output criterion for stability, the system was considered stable if the far field pressure tended toward zero.

Plots of the far field pressure for an impulse noise source are shown below for a number of different conditions of system gain. When G11 is set to -5000, and all the other

gains to 0, the output is that shown in the top plot of figure 5-4. This system is the single loop, single noise source case, discussed in the previous chapter, where the noise source, microphone and attenuating source are all closely spaced. The middle plot of figure 5-4 shows the far field pressure when G22 is set to -5000, and the remaining gains set to 0. This situation is again the single attenuating loop system, with the microphone to attenuating source spacing the same, but located a distance from the noise source. The margin of stability should remain the same, but the attenuation should be much less. The plot shows that stability is unchanged, but does not give any indication of the amount of attenuation achieved. That question is addressed later in the chapter.

When both G11 and G22 are set to -5000, and the other gains to 0, the curve shown in the bottom plot of figure 5-4 results. Using the number of oscillations required for the system output to return to zero as a criterion for stability, this system seems to have a smaller margin of stability than the single loop systems. This system corresponds to the situation in which two attenuating systems are placed in close proximity to one another, with no electrical connection between them. The curves indicate that the bringing together of two stable attenuating loops tends to make them less stable.

There exists the possibility that by cross connecting

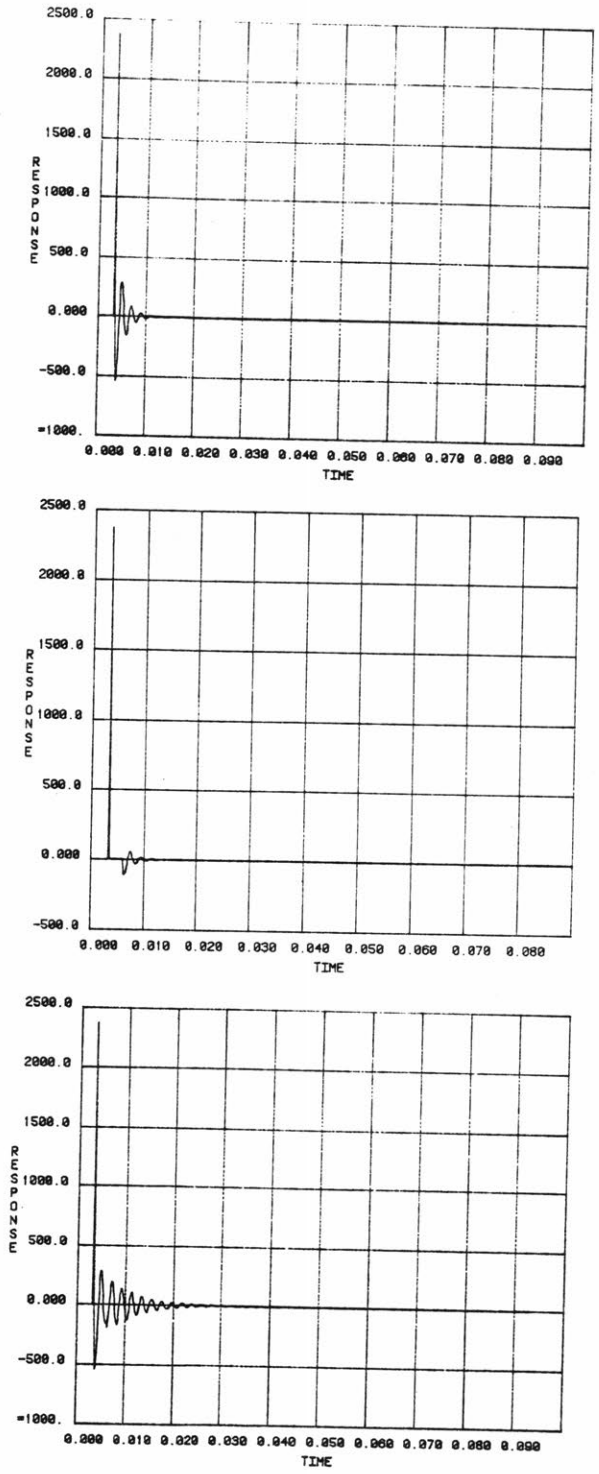


Figure 5-4. Model impulse response. Top plot: G11 = -5000, G12 = G21 = G22 = 0. Middle plot: G22 = -5000, G11 = G12 = G21 = 0. Bottom plot: G11 = G22 = -5000, G21 = G12 = 0.

the two systems, better performance and stability might result. This cross connection is provided by means of G12 and G21. This possibility can be tested using the computer model. First examining the cross loops individually, G12 is set to -25000, which gives the same loop gain as the previous loops, due to the additional attenuation in the longer cross loop air paths. The system is clearly unstable, as shown by the top plot in figure 5-5. This instability is not surprising, considering the additional phase introduced in the loop by the longer air path lengths. If G12 is reduced to -5000, the system impulse response is shown in the middle plot of figure 5-5. The system is now stable. When G21 is set to -5000, with the other gains set to 0, again, a stable system results. However, if both G12 and G21 are set to -5000, the the two previously stable loops become unstable. Even when both G12 and G21 are reduced to -1750, the system remains unstable, as shown in the bottom plot of figure 5-5.

If all four gains are made non-zero, a better idea of the effect of the cross connections on stability can be obtained. Figure 5-6 shows a series of impulse responses for this system. G11 and G22 are held at -5000, while G21 and G12 are set at values from -1000 to +2000. In each case, the effect of adding the cross loop gain is to reduce stability.

So, while the cross connections do not help stability, there is the possibility that they might improve the amount of attenuation realized. In order to answer this question,

the noise source excitation was changed to a sine wave at a frequency of 300 radians/second.

Plots of the far field pressure are shown in figures 5-7 and 5-8. The top plot in figure 5-7 shows the output with all system gains set to zero, resulting in no attenuation. The middle plot shows the far field pressure when G11 = -5000, which represents one attenuating loop operating on the noise source. The bottom plot in figure 5-7 shows the output when G22 = -5000, again a single loop situation, but one in which the noise and attenuating source are separated. In the first case, a reduction of 15 db is obtained, while in the second, only 1 db. Due to the source separation, little attenuation is achieved.

When both G11 and G22 are set to -5000, the far field pressure is shown in the top plot of figure 5-8. The addition of the second attenuating loop has a significant effect on the far field pressure, increasing the amount of attenuation from 15 to 18 db. With G11 and G22 set to -5000, and positive gains assigned to the cross loops, less attenuation is obtained, as seen in the middle plot of figure 5-8. If negative gain is used in the cross loops, some additional attenuation is achieved, but at the cost of greatly reduced stability, as shown in the bottom plot of figure 5-8. Nearly 20 db of attenuation can be realized with G12 and G21 set to -1000, but even a small amount of additional gain causes the system to become unstable.

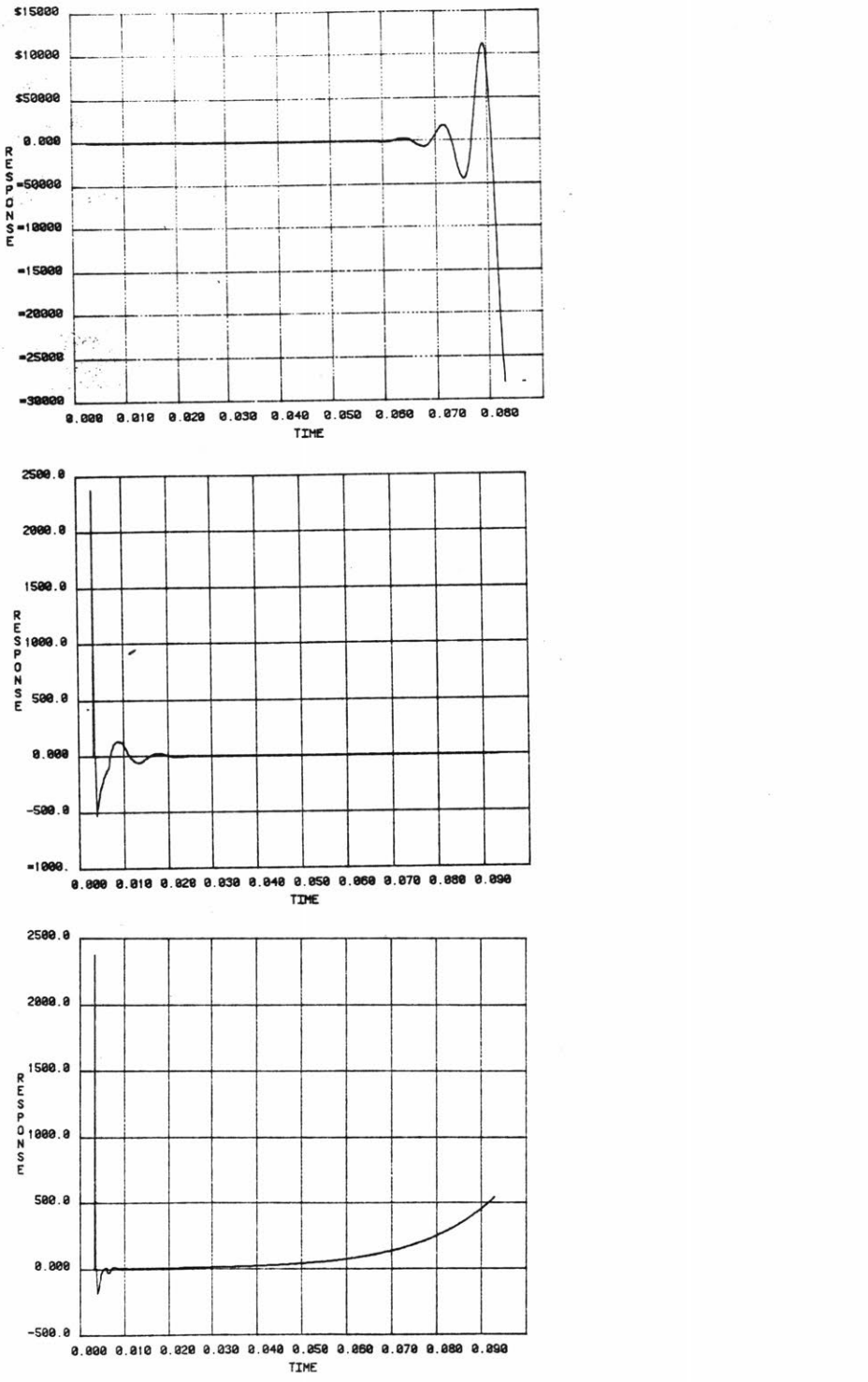


Figure 5-5. Model impulse response. Top plot: G12 = -25000, G11 = G21 = G22 = 0. Middle plot: G12 = -5000, G11 = G21 = G22 = 0. Bottom plot: G12 = G21 = -1750, G11 = G22 = 0.

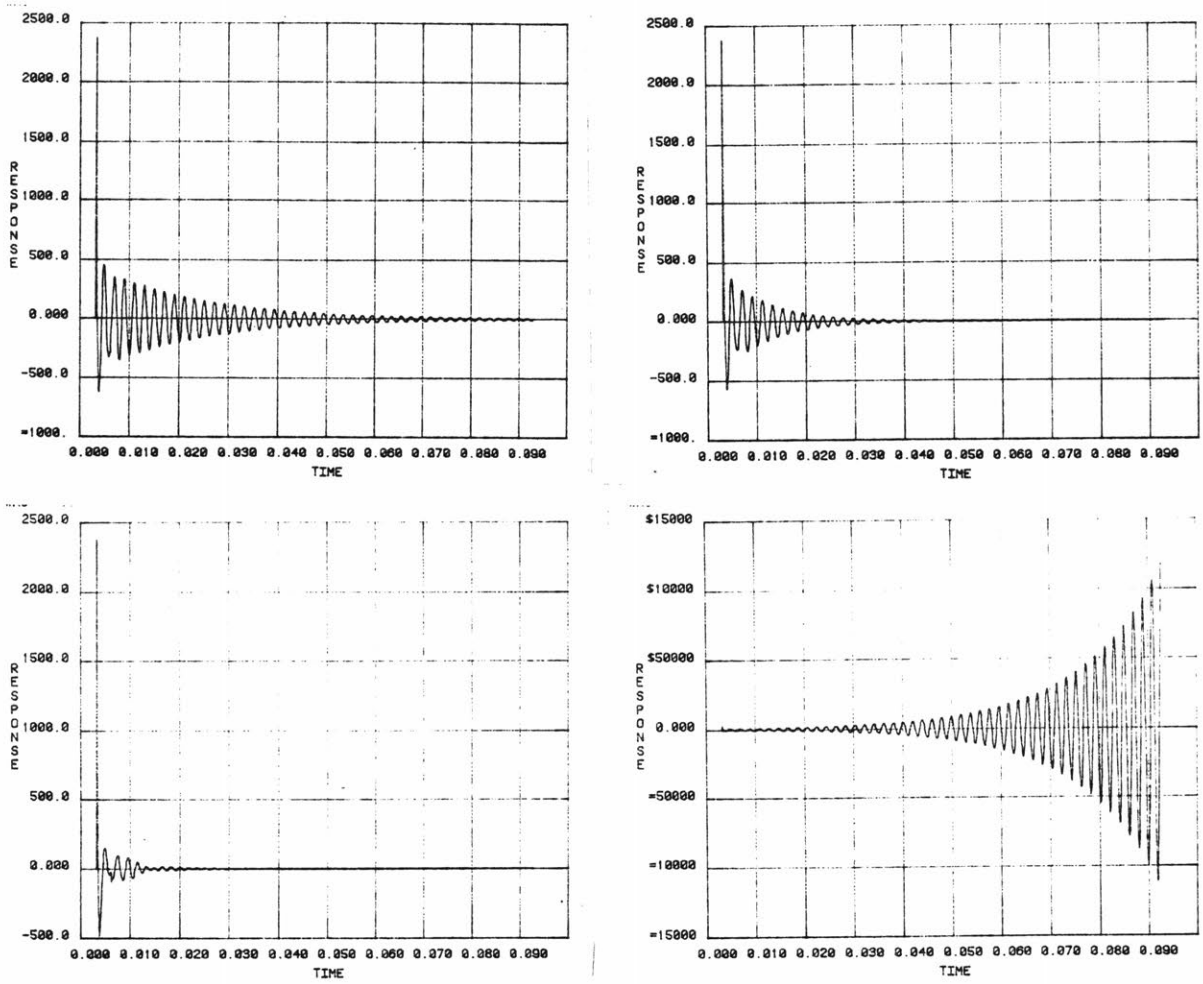


Figure 5-6. Model impulse response. G11 = G22 = -5000. Top left plot: G12 = G21 = -1000. Top right plot: G12 = G21 = -500. Bottom left plot: G12 = G21 = +1000. Bottom right plot: G12 = G21 = +2000.

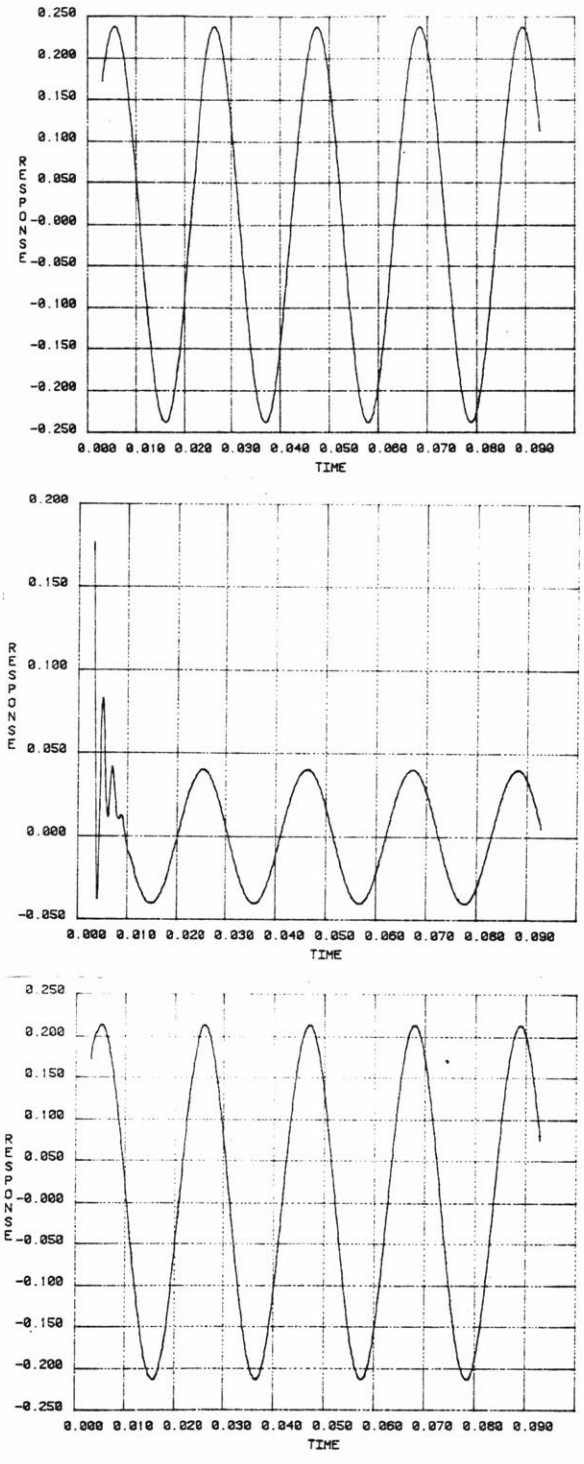


Figure 5-7. Far field pressure predicted by model with sine wave excitation. Top plot: G11 = G12 = G21 = G22 = 0. Middle plot: G11 = -5000, G12 = G21 = G22 = 0. Bottom plot: G22 = -5000, G11 = G12 = G21 = 0.

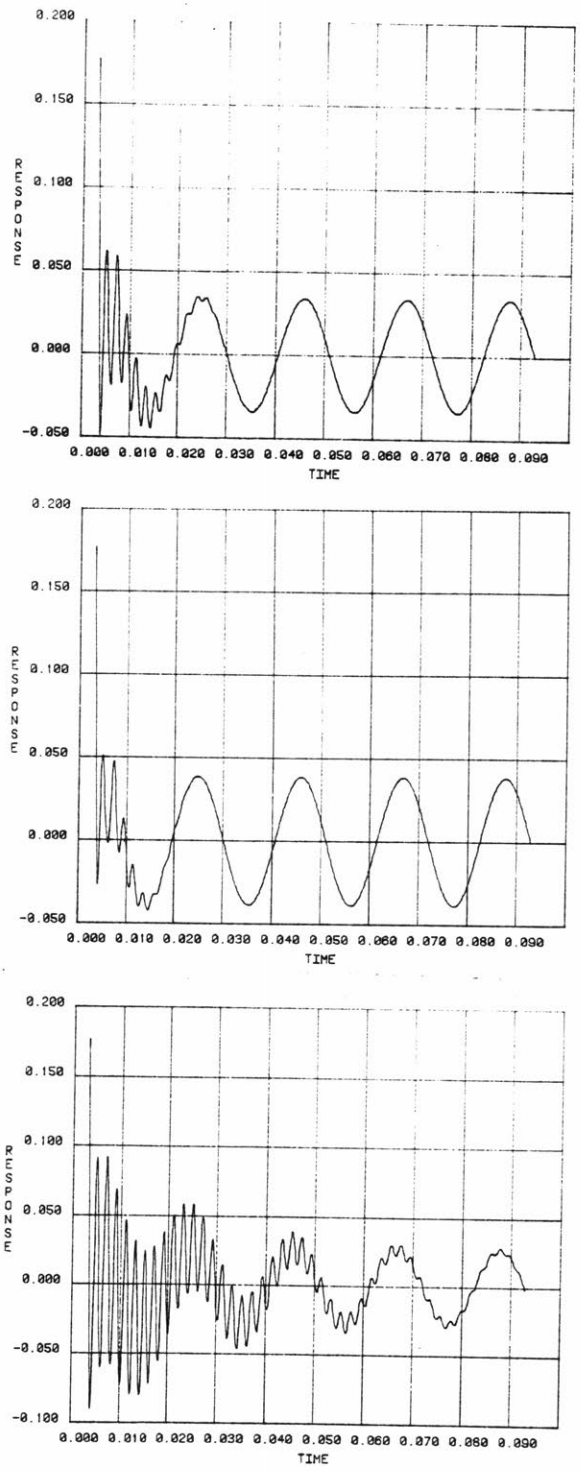


Figure 5-8. Far field pressure predicted by model with sine wave excitation. G11 = G22 = -5000. Top plot: G12 = G21 = 0. Middle plot: G12 = G21 = +500. Bottom plot: G12 = G21 = -1000.

In summary, the addition of a second attenuating loop tends to make the complete system more unstable while improving the amount of attenuation that can be provided. If a single loop system is designed using classical control methods, as described in the previous chapter, and then placed in operation near a similar loop, the stability of the two systems will be impaired. If the individual loops are designed with a reasonable stability margin, however, this impairment need not be a problem.

The model also shows that the addition of cross connections between the two loops provides little additional attenuation. These results are not unexpected. As shown earlier, a second attenuating loop can provide a substantial improvement in attenuation. However, the cross gains create loops with long time delays, resulting in less stability and less potential for attenuation. Therefore, there seems to be little reason to employ the cross loops.

So far, the question of locating the attenuating sources has not been discussed. A detailed answer depends completely on the geometry of the problem at hand, as can be seen from the equation for radiation from sources developed in Appendix 1. However, the closer the attenuating source can be placed to the noise source, the better the attenuation that can be provided.

To verify that two attenuating loops can be stable and

effective with large noise sources, a second attenuating system was built in the lab, identical to the one described in Chapter 4. Together, these two loops were used to attenuate noise from several sources. The experiments were done in the same room as described previously, with the same sources, and in an identical manner.

The first noise source was the Bose model 802 loudspeaker. One attenuating source was placed 0.1m in front of one group of four drivers in the loudspeaker, and the other 0.1m from the other group of four drivers. The measured reverberant field pressure is shown in figure 5-9. A maximum of 12 db of attenuation was attained, at 60 Hz, as compared to the 8 db of attenuation obtained with a single attenuation loop. Noise reduction was observed over a wider frequency band as well, with attenuation from 40 to 200 Hz.

The air compressor was also measured again. One attenuating source was placed next to each cylinder head, approximately 0.1m from the surface of the machine. The measured reverberant field pressure is shown in figure 5-10. In this case, the attenuation increased from 5 db using one attenuator to 8 db using two. Again, attenuation was observed over a wider band of frequencies.

In the laboratory, experimental results tend to back up the results predicted by the derivations and computer models used in this chapter. The addition of a second attenuating source can significantly improve the amount of attenuation

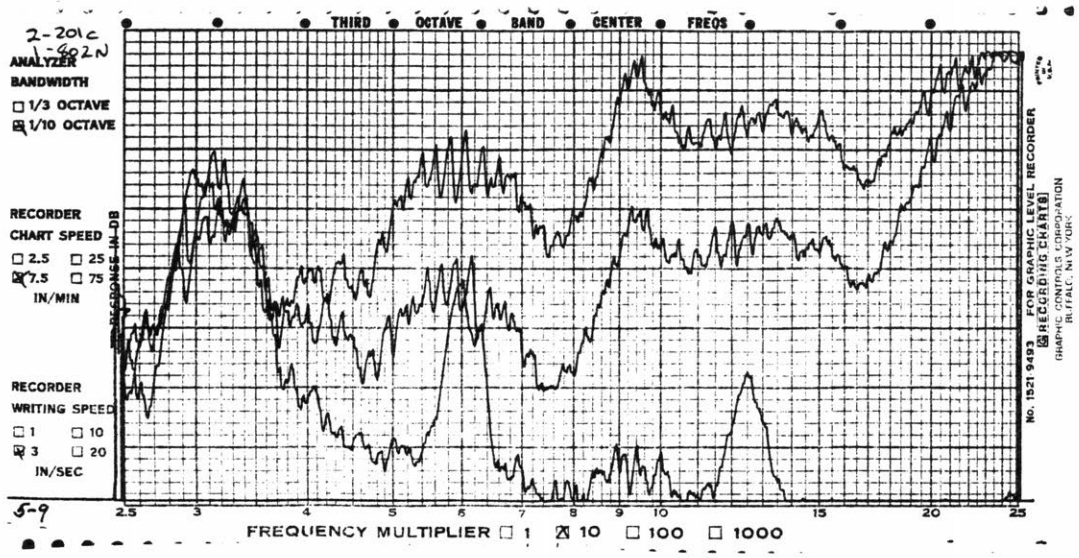


Figure 5-9. Measured reverberant field pressure for Bose 802 speaker noise source. Top curve: noise source operating alone. Middle curve: noise source and two attenuating sources operating. Bottom curve: no sources operating.

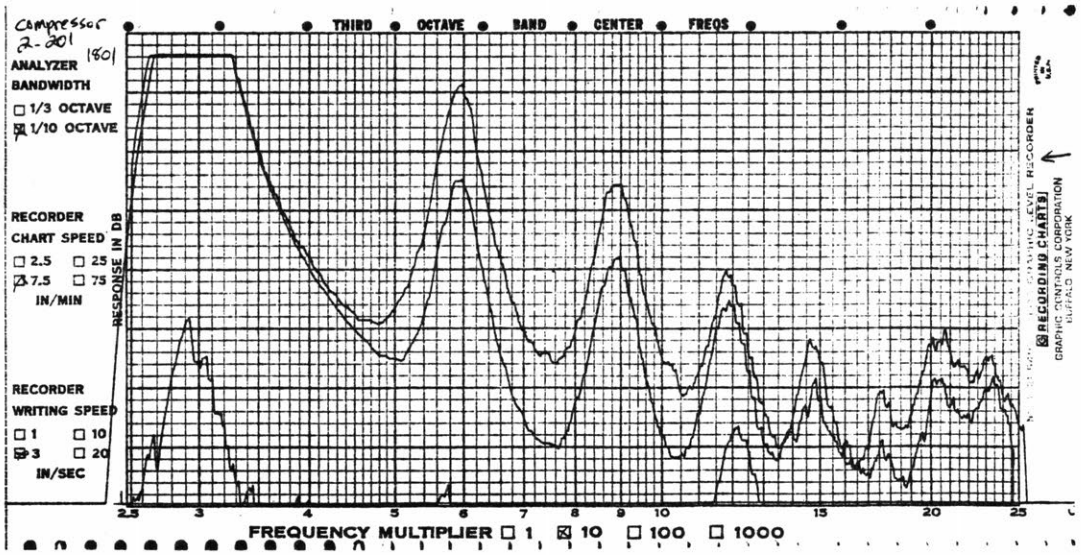


Figure 5-10. Measured reverberant field pressure for air compressor noise source. Top curve: noise source operating alone. Middle curve: noise source and two attenuating sources operating. Bottom curve: no sources operating.

obtained from a large noise source, and can do so without significantly compromising the stability of either individual loop.

# Chapter 6

# SUMMARY
# AND CONCLUSIONS

A new method for globally reducing the power radiated by a noise source has been examined. Equations governing this method were derived. For a simple system, a model was developed in order to predict system performance. Based on this model, a device was constructed and tested in the lab, which performed to within 2 db of the theoretical maximum for this system. A more complicated system, using multiple attenuating loops, was proposed, and a model developed to study system stability and performance. Based on this model, a multiple loop system was built and tested, showing that a multiple loop system could be stable and could improve performance.

A number of practical limitations which could limit the possible applications for this system have been noted throughout this work. The first is the limited amount of noise reduction this system can provide. Under ideal conditions, this system is limited to about 20 db of attenuation at 50 Hz for a 0.1m source spacing. While this

amount of attenuation is hardly insignificant, especially when one considers how difficult it is to attenuate noise to this degree passively, it does represent an absolute maximum. Typical systems, such as the ones built in the lab, only approach this limit for typical noise sources, due in large part, it is suspected, to the size and acoustic complexity of the noise source.

Another difficulty that was experienced in the lab was the limitation that loudspeaker displacement places on the system. If a loudspeaker with either greater displacement capabilities, or with the capability to create more volume velocity with the same displacement, could be used, attenuation could be obtained to a much lower frequency, increasing the usefulness of the system.

Also, both speaker displacement and available amplifier power limit the intensity of sounds that can be attenuated. In the experiments performed with the system, the noise sources used created sound pressure levels of 70 to 80 db in the reverberant field. Obtaining noise attenuation using the experimental speaker and power amplifier described above was not a problem at these sound levels. As discussed, most of the loudspeaker displacement was caused by the system attempting to reduce the 5 to 10 Hz noise present in the room not due to any localized noise source. So speaker displacement due to the level of the noise source being attenuated was not a serious difficulty. However, for the

case of the air compressor, amplifier power was. When the compressor was turned on, the power amplifier would frequently clip while trying to drive the attenuating loudspeaker sufficiently to attenuate the noise. The ten watt amplifier being used had to be replaced with an amplifier capable of approximately 30 watts in order to complete the experiment.

If the noise source were producing in the range of 90 to 100 db SPL in the reverberant field, a not unreasonable level for many applications, significantly higher power amplifiers, and loudspeakers capable of higher volume velocities would be needed. Fortunately, these requirements can be reduced by using a number of attenuating loops. Not only would they probably provide better attenuation for a typical source, but the requirements on power and displacement for each loop would be relaxed.

Another factor which limited the amount of attenuation realized in the lab was the system compensation used. No claim is made that the compensation used is optimal. Better compensation might exist which could provide significantly more open loop gain. Whereas this gain might not increase the maximum amount of attenuation, which already approaches the theoretical maximum, it could increase the amount of attenuation for frequencies above and below that for which the maximum occurs, thus improving the overall system performance. In addition, no really good method of

developing a compensation scheme for multiple loop systems was developed. This step will probably have to await further developments in the control theory field. But it seems likely that improved performance is possible by developing a compensator especially for multiple loop systems.

Despite these limits, it is believed that the system proposed here could have practical applications for attenuating low frequency noise.

# Appendix 1

## MULTIPLE SOURCE
## RADIATED POWER DERIVATION

In Chapter 3, an equation for the power radiated from two arbitrary point sources was derived. In this appendix, the power radiation equations for three point sources will be derived, and then generalized to N point sources.

The geometry of the problem is shown in figure A1-1, and follows that of the problem of multiple attenuating sources discussed in Chapter 5. A noise point source is located at the origin, having volume velocity $\underline{Vvn}$, of magnitude Vvn and phase angle zero. One attenuating point source is located at $(r_1,0)$ in polar coordinates, and the other at $(r_2,\theta_2)$. The sources have volume velocity magnitudes of $Vvc_1$ and $Vvc_2$ respectively, and phase angles $\psi_1$, and $\psi_2$. A distant observer is located at $(r,\theta)$.

As before, the pressure at the observer can be written as the sum of pressures due to the three sources,

$$\underline{P} = \frac{j f \rho_o}{2} \frac{Vvn \exp(-jkr)}{r}$$

$$+ \frac{Vvc_1 \exp(j\psi_1) \exp(-jk(r-r_1\cos\theta))}{r - r_1\cos\theta}$$

$$+ \frac{Vvc_2 \exp(j\psi_2) \exp(-jk(r-r_2\cos(\theta-\theta_2))}{r - r_2\cos(\theta-\theta_2)} \qquad (A1.1)$$

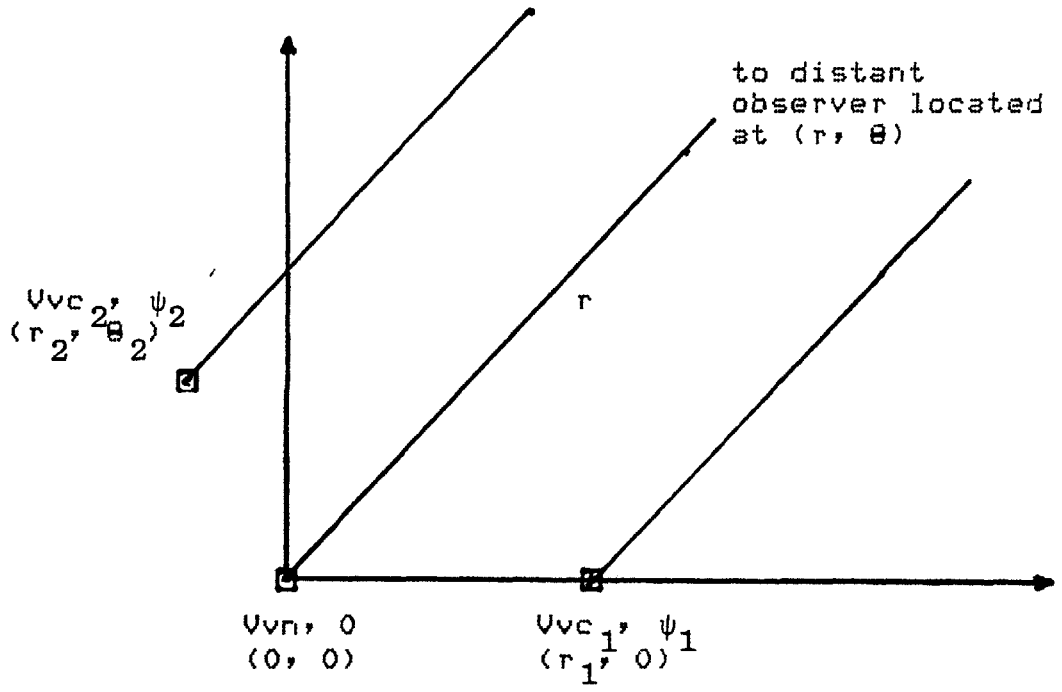


Figure A1-1. Geometry of the three point source problem.

Approximating the denominator terms by r, and regrouping gives

$$\underline{E} = \frac{J f \rho_o \exp(-Jkr)}{2r}\{Vvn + Vvc_1 \exp(J(\psi_1+kr_1\cos\theta)) + Vvc_2 \exp(J(\psi_2+kr_2\cos(\theta-\theta_2))\} \qquad (A1.2)$$

Separating into real and imaginary parts and squaring to find magnitude squared yields

$$|\underline{E}|^2 = \frac{f^2\rho_o^2}{4r^2}\{ \{Vvn + Vvc_1 \cos(\psi_1+kr_1\cos\theta) + Vvc_2 \cos(\psi_2 + kr_2\cos(\theta-\theta_2))\}^2 + \{ Vvc_1 \sin(\psi_1 + kr_1\cos\theta) + Vvc_2 \sin(\psi_2 + kr_2\cos(\theta-\theta_2))\}^2 \} \qquad (A1.3)$$

Making the substitutions

$$\alpha = k\, r_1 \cos\theta_1 \qquad (A1.4)$$

and

$$\beta = k\, r_2 \cos(\theta-\theta_2) \qquad (A1.5)$$

gives

$$|\underline{E}|^2 = \frac{f^2\rho_o^2}{4r^2}\{(Vvn + Vvc_1 \cos(\psi_1+\alpha) + Vvc_2 \cos(\psi_2+\beta))^2 + (Vvc_1\sin(\psi_1+\alpha) + Vvc_2 \sin(\psi_2+\beta))^2\} \qquad (A1.6)$$

which reduces to

$$|\underline{p}|^2 = \frac{f^2 \rho_o^2}{4r^2} \{ Vvn^2 + Vvc_1^2 + Vvc_2^2$$

$$+2\, Vvc_1\, Vvc_2 \cos(\psi_1-\psi_2+\alpha-\beta)$$

$$+ 2\, Vvn\, Vvc_1 \cos(\psi_1+\alpha)$$

$$+ 2\, Vvn\, Vvc_2 \cos(\psi_2+\beta) \} \qquad (A1.7)$$

Power is related to the surface integral of the pressure magnitude squared

$$P \propto \int_0^{\pi} \int_0^{2\pi} |\underline{p}|^2\, r^2 \sin\phi \, d\theta \, d\phi \qquad (A1.8)$$

Since there is no $\phi$ dependence, this reduces to

$$P \propto \int_0^{2\pi} |\underline{p}|^2 \, d\theta \qquad (A1.9)$$

which becomes

$$P \propto \int_0^{2\pi} \{Vvn^2 + Vvc_1^2 + Vvc_2^2\} \, d\theta$$

$$+ \int_0^{2\pi} 2\, Vvc_1\, Vvc_2 \cos(\psi_1-\psi_2+\alpha-\beta) \, d\theta$$

$$+ \int_0^{2\pi} 2\, Vvn\, Vvc_1 \cos(\psi_1+\alpha) \, d\theta$$

$$+ \int_0^{2\pi} 2\, Vvn\, Vvc_2 \cos(\psi_2+\beta) \, d\theta \qquad (A1.10)$$

This integral can be evaluated term by term. The first term reduces to

$$\int_0^{2\pi} (Vvn^2 + Vvc_1^2 + Vvc_2^2)\, d\theta$$

$$= 2\pi\,(Vvn^2 + Vvc_1^2 + Vvc_2^2) \qquad \text{(A1.11)}$$

The second term

$$\int_0^{2\pi} 2\, Vvn\, Vvc_1 \cos(\psi_1+\alpha)\, d\theta \qquad \text{(A1.12)}$$

may be rewritten

$$2\, Vvn\, Vvc_1 \{ \int_0^{2\pi} \cos\psi_1 \cos\alpha\, d\theta - \int_0^{2\pi} \sin\psi_1 \sin\alpha\, d\theta \} \qquad \text{(A1.13)}$$

Substituting for $\alpha$ gives

$$2\, Vvn\, Vvc_1 \{ \cos\psi_1 \int_0^{2\pi} \cos(kr_1 \cos\theta)\, d\theta$$

$$-\sin\psi_1 \int_0^{2\pi} \sin(kr_1 \cos\theta)\, d\theta \} \qquad \text{(A1.14)}$$

As in Chapter 3, the term kr is always small at frequencies of interest, so the series expansions for sine and cosine may be used, and the higher order terms dropped.

$$\cos(kr\cos\theta) = 1 - \frac{k^2 r^2 \cos^2\theta}{2} + \ldots \qquad \text{(A1.15)}$$

$$\sin(kr\cos\theta) = kr\cos\theta + \ldots \qquad \text{(A1.16)}$$

This substitution gives

$$2\ Vvn\ Vvc_1\{\ \cos\psi_1 \int_0^{2\pi} \left(1 - \frac{k^2 r_1^2 \cos^2\theta}{2}\right) d\theta$$

$$- \sin\psi_1 \int_0^{2\pi} (kr_1\cos\theta)\ d\theta\ \} \qquad (A1.17)$$

which reduces to

$$2\pi\ Vvn\ Vvc_1\ \cos\psi_1 \left(\ 2 - \frac{k^2 r_1^2}{2}\ \right) \qquad (A1.18)$$

The third term

$$\int_0^{2\pi} 2\ Vvn\ Vvc_2\ \cos(\psi_2+\beta)\ d\theta \qquad (A1.19)$$

may be handled in an identical manner, and reduces to

$$2\pi\ Vvn\ Vvc_2\ \cos\psi_2 \left(2 - \frac{k^2 r_2^2}{2}\right) \qquad (A1.20)$$

The fourth term

$$\int_0^{2\pi} 2\ Vvc_1\ Vvc_2\ \cos((\psi_1-\psi_2)+(\alpha-\beta))\ d\theta \qquad (A1.21)$$

can be rewritten

$$2\ Vvc_1\ Vvc_2\ \{\cos(\psi_1-\psi_2) \int_0^{2\pi} \cos(\alpha-\beta)\ d\theta$$

$$- \sin(\psi_1-\psi_2) \int_0^{2\pi} \sin(\alpha-\beta)\ d\theta\ \} \qquad (A1.22)$$

These two integrals can be evaluated independently. The first one

$$\int_0^{2\pi} \cos(\alpha-\beta)\, d\theta \qquad \text{(A1.23)}$$

expands to

$$\int_0^{2\pi} \cos(k(r_1\cos\theta - r_2\cos(\theta-\theta_2)))\, d\theta \qquad \text{(A1.24)}$$

when the substitutions are made. Using the series expansion for cosine and dropping higher order terms,

$$\int_0^{2\pi} 1 - \frac{k^2}{2}\left( r_1^2 \cos^2\theta + r_2^2 \cos^2(\theta-\theta_2) - 2r_1r_2 \cos\theta \cos(\theta-\theta_2)\right) d\theta \qquad \text{(A1.25)}$$

This integral becomes

$$2\pi - \frac{k^2}{2}\left( r_1^2\pi + r_2^2\pi - 2\pi\, r_1r_2 \cos\theta_2\right) \qquad \text{(A1.26)}$$

which reduces to

$$2\pi - \frac{\pi k^2}{2}(r_{12}^2) \qquad \text{(A1.27)}$$

where $r_{12}$ is the distance between the first and second attenuating source.

The second integral in the fourth term is

$$\int_0^{2\pi} \sin(kr_1\cos\theta - kr_2\cos(\theta-\theta_2))\, d\theta \qquad \text{(A1.28)}$$

Using the series expansion for sine gives

$$\int_0^{2\pi} k\,(r_1\cos\theta - r_2\cos(\theta-\theta_2))\, d\theta \qquad \text{(A1.29)}$$

which has the solution zero. Thus, the entire fourth term becomes

$$2\ Vvc_1\ Vvc_2\ (2\pi - \frac{\pi\ k\ r_{12}}{2})\ \cos(\psi_1-\psi_2) \qquad (A1.30)$$

Putting all four terms together, the final expression for power radiated becomes

$$\begin{aligned} P \propto\ & Vvn^2 + Vvc_1^2 + Vvc_2^2 \\ & + Vvc_1\ Vvc_2\ (2 - \frac{k^2\ r_{12}^2}{2})\ \cos(\psi_1-\psi_2) \\ & + Vvn\ Vvc_1\ (2 - \frac{k^2\ r_1^2}{2})\ \cos\ \psi_1 \\ & + Vvn\ Vvc_2\ (2 - \frac{k^2\ r_2^2}{2})\ \cos\ \psi_2 \end{aligned} \qquad (A1.31)$$

This proportionality solves the problem of chapter 5, with two attenuating sources and one noise source. A problem in chapter 3, however, involved N noise sources and one attenuating source. The expression just derived may be expanded to solve this problem.

Consider an attenuating source at the origin with volume velocity magnitude Vvc and zero phase angle. Throughout space, at distances $r_i$ are noise sources, having volume velocity magnitude $Vvn_i$ and phase $\psi_i$. By examining the three point source solution and expanding it to M point sources, the power radiated can be written

$$P \propto V_{vc}^2 + \sum_{i=1}^{M} V_{vn_i}^2 + V_{vc} \cdot \sum_{i=1}^{M} V_{vn_i} \left( 2 - \frac{k^2 r_i^2}{2} \right) \cos\psi_i$$

$$+ \sum_{\substack{i=1 \\ i \neq j}}^{M} \sum_{j=1}^{M} V_{vn_i} V_{vn_j} \left(2 - \frac{k^2 r_{ij}^2}{2}\right) \cos(\psi_i - \psi_j) \qquad (A1.32)$$

This solution may also be expanded to include additional attenuating sources by relabeling some of the noise sources as attenuating sources.

In Chapter 5, the accuaracy of some of the approximations used in the derivations above was questioned. If, in the derivation of the three source power radiated equation, an additional term is retained in both the sine and the cosine expansions, the expression for power radiated becomes

$$P \propto V_{vn}^2 + V_{vc_1}^2 + V_{vc_2}^2$$

$$+ V_{vn} V_{vc_1} \left(2 - \frac{k^2 r_1^2}{2} + \frac{k^4 r_1^4}{16}\right) \cos \psi_1$$

$$+ V_{vn} V_{vc_2} \left(2 - \frac{k^2 r_2^2}{2} + \frac{k^4 r_2^4}{16}\right) \cos \psi_2$$

$$+ V_{vc_1} V_{vc_2} \left(2 - \frac{k^2 r_{12}^2}{2}\right.$$

$$+ k \left\{ \frac{r_1^4}{16} + \frac{r_2^4}{16} + \left( \frac{r_1^3 r_2}{4} + \frac{r_1 r_2^3}{4} \right) \cos \theta_2 \right.$$

$$\left.\left. + \frac{3 r_1^2 r_2^2}{8} \left( \frac{\cos^2 \theta_2}{2} + 1 \right) \right\} \right) \cos(\psi_1 - \psi_2) \qquad \text{(A1.33)}$$

In general, the additional terms provide little improvement in accuracy, but for some situations, such as the geometry discussed in Chapter 5, those terms are essential.

# Appendix 2

## ATTENUATION OF MORE COMPLEX SOURCES

Throughout much of the discussion, point acoustic sources have been assumed. It was shown that a loudspeaker can be reasonably modeled by a point source for frequencies over which the attenuator system operates. However, noise sources may not be so conveniently modeled. The device producing the noise may be much larger than a wavelength, in which case a single attenuating system can not produce much attenuation. A more interesting situation is one in which the noise source may be modeled by a number of point sources at varying small distances, and with varying phases and magnitudes.

To get an indication of the amount of noise attenuation that can be expected for some collections of point sources, the equation developed in Appendix 1 may be used.

$$P \propto Vvc^2 + \sum_{i=1}^{M} Vvn_i^2 + Vvc \cdot \sum_{i=1}^{M} Vvn_i \left( 2 - \frac{k^2 r_i^2}{2} \right) \cos\psi_i$$

$$+ \sum_{\substack{i=1 \\ i \neq j}}^{M} \sum_{j=1}^{M} Vvn_i \, Vvn_j \left(2 - \frac{k^2 r_{ij}^2}{2}\right) \cos(\psi_i - \psi_j) \qquad \text{(A2.1)}$$

Power radiated by M noise sources at distance r , with magnitude $Vvn_i$ and phase $\psi_i$, and one attenuation source at the origin having magnitude Vvc and phase 0.

This equation will be applied first to a dipole source. The dipole consists of two point sources, each having volume velocity magnitude equal to one, but with a phase difference of 180 degrees, separated by one twentieth of a wavelength. Substituting these values into equation (A2.1), a radiated power of -13 db is obtained, where zero db refers to the power radiated by a single point source having a volume velocity of one. If an attenuating source having volume velocity magnitude Vvc and phase $\psi$ is placed equidistant from both of the sources making up the dipole, the power radiated becomes

$$1 + 1 + Vvc^2 + Vvc \left(2 - \frac{\pi^2}{200}\right) \cos(180 - \psi)$$

$$- \left(2 - \frac{\pi^2}{200}\right) + Vvc \left(2 - \frac{\pi^2}{200}\right) \cos\psi \qquad \text{(A2.2)}$$

which reduces to

$$Vvc + \frac{\pi^2}{200} \qquad (A2.3)$$

The minimization in this case results in setting Vvc = 0. So in the situation where an attenuating source is placed at the midpoint between two sources making up a dipole, no attenuation can be expected using this system.

A different attenuation source position may provide more interesting results. Assume that the dipole remains unchanged, but that the attenuator source is placed one twentieth of a wavelength away from one of the sources making up the dipole such that the three sources form a line. Now, the equation for power radiated becomes

$$1 + 1 + Vvc^2 - Vvc\,(2 - \frac{\pi^2}{50})\cos\psi$$

$$- (2 - \frac{\pi^2}{200}) + Vvc\cos\psi\,(2 - \frac{\pi^2}{200}) \qquad (A2.4)$$

which reduces to

$$Vvc\cos\psi\,(\frac{3\pi^2}{200}) + \frac{\pi^2}{200} + Vvc \qquad (A2.5)$$

Minimizing this equation gives a volume velocity

$$Vvc = \frac{3\pi^2}{400}$$

and a phase of 180 degrees, which yields a power of -13.1 db, or one tenth of one db less than the previous case.

From these calculations, it becomes apparent that using this attenuation scheme on dipole sources will not produce any significant attenuation. Since the attenuator system

attempts to make a dipole out of the noise source and the attenuating source, then if the noise source is a dipole, this scheme will not significantly reduce the power radiated by the dipole.

A collection of point sources for which the attenuator is effective is a set of four in phase point souces, each equidistant from the origin, and equally spaced about it. If each source has a volume velocity magnitude of 1 and a phase angle of 0, and each is located one twentieth of a wavelength from the next, then the total power radiated is

$$4 + 12 - \frac{6\pi^2}{200} \qquad (A2.6)$$

which is 12.0 db. If an attenuating source of magnitude Vvc and phase  is located at the origin, the power radiated is

$$Vvc^2 + 4 + 12 + - \frac{6\pi^2}{200} + 4\ (2 - \frac{\pi^2}{400})\ Vvc\ \cos\psi \qquad (A2.7)$$

Minimizing this equation gives a volume velocity

$$Vvc = 4 - \frac{\pi^2}{100}$$

and phase of 180 degrees, yielding a total power radiated of -13.1 db. Thus, in this situation, a power reduction of 25 db can be attained.

These calculations show that the attenuation scheme proposed can effectively reduce acoustic power radiated for at least some non-point sources of noise, but that for others, such as a dipole, little or no attenuation can be

expected, due to the method of attenuation that is used.

# Appendix 3

## ELECTRICAL MODELS OF LOUDSPEAKERS

In order to model the attenuation system so that its performance may be predicted, an electrical model for the various elements of the system must be developed. For the loudspeaker, the model developed in Beranek (1), as shown in figure A3-1, will be used.

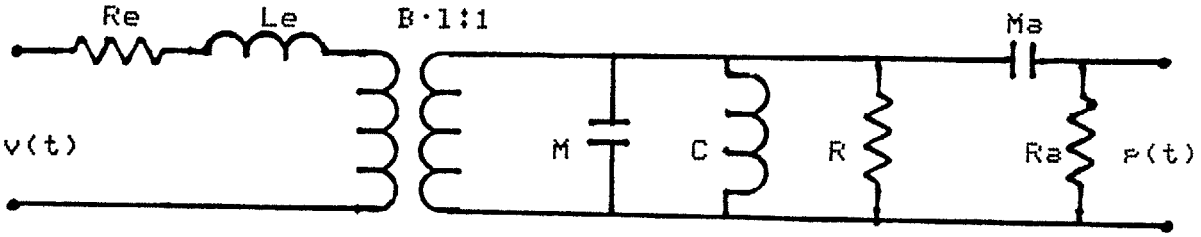


Figure A3-1. Loudspeaker model.

Re and Le represent the electrical resistance and inductance of the speaker's voice coil and electrical wiring. M, C, and R represent the mechanical mass, compliance, and resistance of the loudspeaker cone, spider, and air loading due to the enclosure. Ra and Ma represent an approximation to the acoustic impedance seen by the speaker. A transformer with a turns ratio of B·1 to 1, the product of the magnetic

flux times the length of voice coil wire in the air gap, connects the electrical and mechanical sections of the model.

The acoustic parameters may be calculated using Beranek's (1) table 5-1, but the others must be measured. Measurement of some of the parameters might be difficult, but fortunately, all of them may be derived from two simple electrical measurements. First, the model can be redrawn as shown in figure A3-2, removing the acoustic elements and the transformer, and scaling the other elements as needed.

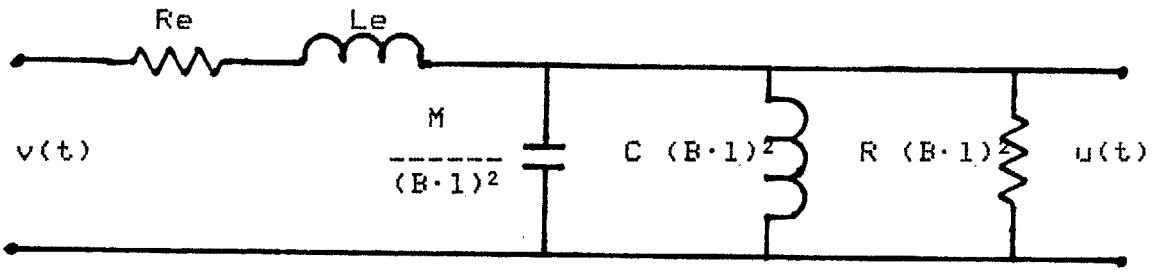


Figure A3-2. Simplified loudspeaker model.

For the experimental loudspeaker used as the attenuating source, a DC resistance of 3.5 ohms was measured. Thus, Re can be immediately set to 3.5 ohms. An impedance curve was run, which is shown in figure A3-3. (The curve with the higher frequency peak is the one of interest at the moment. The other curve will be used later in these calculations.) The impedance peaks at the resonant frequency, $f_o$ = 74 Hz. At some frequency, the curve begins to rise with a slope of approximately 4 db per octave. (The slope is 4, rather than 6 db per octave, due to the skin effect in the pole piece.

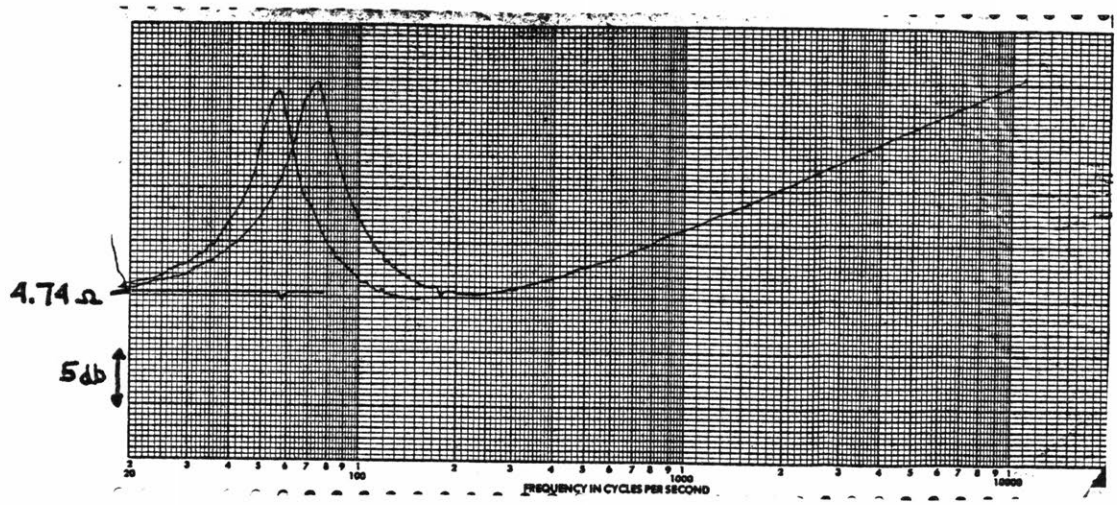


Fisure A3-3. Measured impedance curves for the experimental loudspeaker.

This effect was neslected in makins the electrical model since the model was used only at frequencies below those for which the effect is important.) The rise in impedance is due to the interaction between Re and Le. The break frequency can be read off the impedance curve as beins 500 Hz, and Le can be calculated to be 1.23 mH.

The resonant peak is due to the interaction between M and C. The frequency of this peak, $f_o$ may be written

$$f_o = \frac{1}{2\pi \sqrt{MC}} \qquad (A3.1)$$

If additional mass is added to the cone, the resonant frequency will decrease to

$$f_o' = \frac{1}{2\pi\sqrt{(M + \Delta m)C}} \qquad (A3.2)$$

These two equations may be combined to give an expression for mass which depends only on the two resonant frequencies and the added mass.

$$M = \Delta m \frac{(f_o')^2}{(f_o)^2 - (f_o')^2} \qquad (A3.3)$$

The second curve in figure 3-3 is the impedance of the speaker with an additional ten grams of mass added to the cone. From the two curves $f_o$ is found to be 74 Hz, and $f_o'$ 56 Hz. These values result in a mass of 13.4g. Substituting this value back into the expression for resonant frequency gives a compliance value of $3.45 \times 10^{-4}$ m/nt.

The Q of the loudspeaker can be written as

$$Q = \frac{Re \quad f_o}{Rpeak\ (f_{-3} - f_{-3})} \qquad (A3.4)$$

Rpeak is the value of the impedance at the resonant frequency, which is 41.98 ohms according to the impedance curve. The frequencies $f_{-3}$ are those for which the impedance is 3db below that at resonance. For this speaker, the frequencies are 66 and 80 Hz. Substituting these values into the expression gives a value of 0.490 for Q. Since Q may also be written

$$Q = \frac{2\pi f_o M Re}{(B \cdot l)^2} \qquad (A3.5)$$

the B·l product squared is be found to be 49.5. The peak resistance may be written

$$Rpeak = R (B \cdot l)^2 + Re \qquad (A3.6)$$

So, the value of R, mechanical resistance, may be calculated, which is 0.77 mechanical ohms.

Lastly, the values for acoustical elements may be calculated using Beranek's (1) table 5-1. Summarizing, the values for the electrical model of the attenuator loudspeaker are:

$Re = 3.89$
$Le = 1.23 \times 10^{-3}$

$B\ l = 7.03$

$R = 0.77$
$M = 1.34 \times 10^{-2}$
$C = 3.45 \times 10^{-4}$

$Ra = 1.17 \times 10^{-1}$
$Ma = 6.74 \times 10^{-4}$

If this electrical model is analyzed using the computer circuit analysis program, the impedance curve shown in fisure A3-4 is obtained. This curve very closely matches the measured impedance curve for this loudspeaker, indicating that the model accurately reflects the actual speaker.

At extreme low frequencies, air leaks in the speaker enclosure become important. In order to determine if the box leak was at a sufficiently high frequency to be sisnificant, some additional measurements were made.

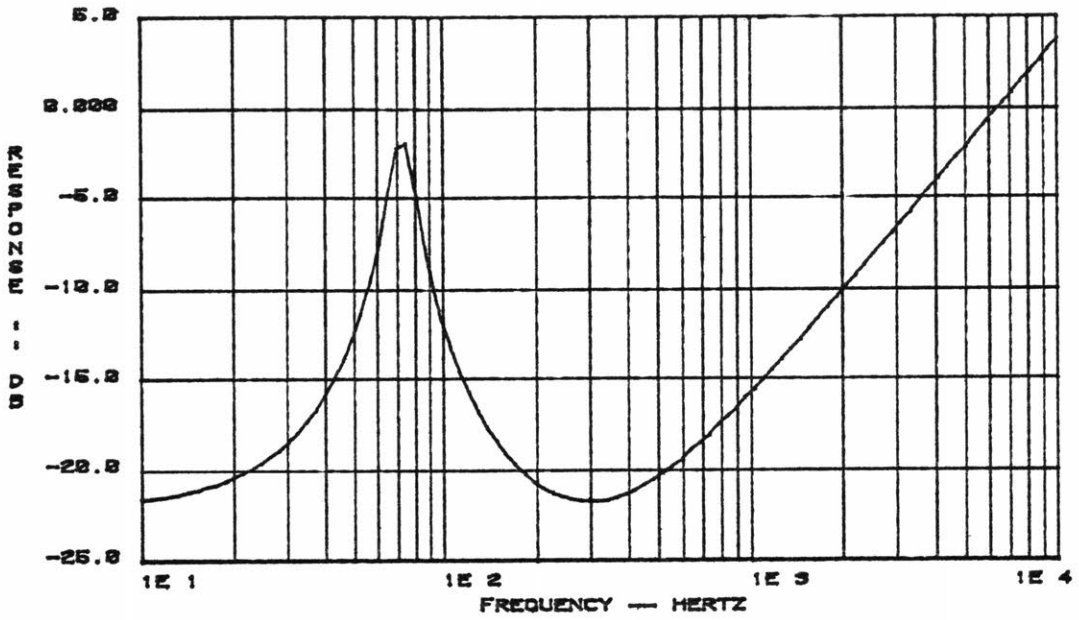


Figure A3-4. Calculated impedance curve for the experimental loudspeaker.

The experimental speaker was excited mechanically, then released, and allowed to relax to its neutral position with its electrical terminals open circuited. The displacement was measured and displayed on an oscilloscope, resulting in the displacement curve shown in figure A3-5. The horizontal scale is 0.5 seconds per division, and the vertical is 1mm per division. Zero displacement is one division from the bottom. The time constant for the box leak can be seen to be approximately 2 seconds, corresponding to a box leak frequency of 0.08 Hz. This frequency was sufficiently low that the box leak was left out of the model.

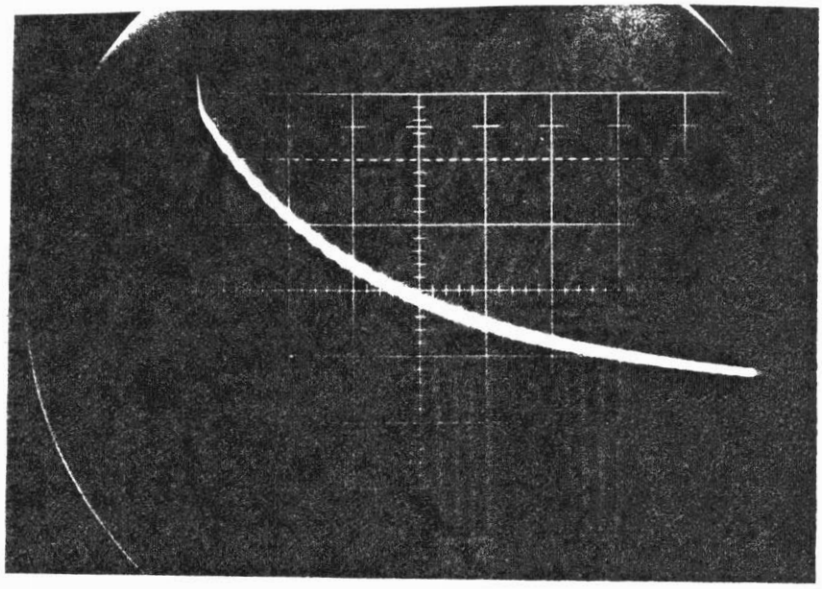

Figure A3-5. Displacement curve for experimental loudspeaker.

# Appendix 4

## COMPUTER PROGRAM

## SOURCE LISTINGS

```
C       PROGRAM TO VERIFY THE MINIMIZATION OF ATTENUATOR OUTPUT.
C       CALCULATES THE POWER OUT FOR A NOISE SOURCE AND ATTENUATING
C       SOURCE OF VARYING MAGNITUDE AND PHASE.
      DIMENSION PSI(101),A1(101),A2(101),A3(101),A4(101),A5(101),VV(5)
      PI=3.14159
      RK2=2.-PI*PI/200
      VV(1)=0.5
      VV(2)=0.89
      VV(3)=1.0
      VV(4)=1.12
      VV(5)=2.0
      DO 100 I=1,101
      PSI(I)=2.*PI*FLOAT(I)/101.
      A1(I)=10.*ALOG10(ABS(1.+VV(1)*VV(1)+COS(PSI(I))*VV(1)*RK2))
      A2(I)=10.*ALOG10(ABS(1.+VV(2)*VV(2)+COS(PSI(I))*VV(2)*RK2))
      A3(I)=10.*ALOG10(ABS(1.+VV(3)*VV(3)+COS(PSI(I))*VV(3)*RK2))
      A4(I)=10.*ALOG10(ABS(1.+VV(4)*VV(4)+COS(PSI(I))*VV(4)*RK2))
      A5(I)=10.*ALOG10(ABS(1.+VV(5)*VV(5)+COS(PSI(I))*VV(5)*RK2))
100   CONTINUE
      PRINT 112
112   FORMAT ('PLOT=1, CRT=0')
      READ (1,*) IP
      CALL ATPL(101,PSI,A1,A2,A3,A4,A5,'PHASE (RAD)~','POWER * DB~',IP)
      STOP
      END
```

```
      SUBROUTINE ATPL(N,X,Y1,Y2,Y3,Y4,Y5,LX,LY,IP)
C     SUBROUTINE TO PLOT 5 CURVES ON SAME SET OF AXES
      DIMENSION X(N),Y1(N),Y2(N),Y3(N),Y4(N),Y5(N),O(2),SB(10)
      O(1)=0.13
      O(2)=0.1
      DX=0.85
      DY=0.85
      PTX=0.0
      PTY=0.0
      CALL REST
      IF (IP .EQ. 1) CALL V10U(1,0)
      CALL BOUND(N,X,SX,BX,UX,PTX)
      CALL BOUND(N,Y1,SB(1),SB(2),UY,PTY)
      CALL BOUND(N,Y2,SB(3),SB(4),UY,PTY)
      CALL BOUND(N,Y3,SB(5),SB(6),UY,PTY)
      CALL BOUND(N,Y4,SB(7),SB(8),UY,PTY)
      CALL BOUND(N,Y5,SB(9),SB(10),UY,PTY)
      CALL BOUND(10,SB,SY,BY,UY,PTY)
      CALL AX(0,O,DX,SX,BX,UX,DY,PTX)
      CALL LABEL(0,O,DX,LX)
      CALL AX(1,O,DY,SY,BY,UY,DX,PTY)
      CALL LABEL(1,O,DY,LY)
      CALL XYDAT(N,X,Y1,SX,BX,UX,SY,BY,UY,O,DX,DY,PTX,PTY)
      CALL XYDAT(N,X,Y2,SX,BX,UX,SY,BY,UY,O,DX,DY,PTX,PTY)
      CALL XYDAT(N,X,Y3,SX,BX,UX,SY,BY,UY,O,DX,DY,PTX,PTY)
      CALL XYDAT(N,X,Y4,SX,BX,UX,SY,BY,UY,O,DX,DY,PTX,PTY)
      CALL XYDAT(N,X,Y5,SX,BX,UX,SY,BY,UY,O,DX,DY,PTX,PTY)
      CALL DRAW(0.0,1.0,0)
      IF (IP .EQ. 1) CALL V10U(-1,0,'CRPLOT')
      RETURN
      END
```

```
C       PROGRAM TO PLOT TOTAL POWER RADIATED BY TWO POINT SOURCES
C       RADIATING WITH SAME VOLUME VELOCITY BUT OPPOSITE SIGNS,
C       LOCATED 0.1 AND 0.2 M APART, COMPARED TO ONE POINT SOURCE
C       HAVING SAME VOLUME VELOCITY.
        DIMENSION FREQ(200),PWR1(200),PWR2(200)
        DO 100 I=1,200
        FREQ(I)=10**(1.+(FLOAT(I))/100.)
        PWR1(I)=10.*ALOG10(ABS(2.-2.*(1.-8.30E-7*FREQ(I)**2)))
        PWR2(I)=10.*ALOG10(ABS(2.-2.*(1.-3.32E-6*FREQ(I)**2)))
100     CONTINUE
        PRINT 110
110     FORMAT ('1=PLOT, 0=CRT')
        READ (1,*) IP
        IF (IP .EQ. 1) CALL V10U(1,0)
        CALL PLOT2(200,FREQ, PWR1,PWR2,'FREQUENCY~','POWER*DB~')
        IF (IP .EQ. 1) CALL V10U(-1,0,'CRPLOT')
        STOP
        END
```

```
C       PROGRAM TO DETERMINE TOTAL POWER RADIATED BASED ON SPEAKER
C       VELOCITY OUTPUT OF TWEAK
C       ***CURRENTLY SET UP FOR SP201 FILES.  NOTE THAT SPECIAL
C       FILES MUST BE USED FOR TWEAK.
      DIMENSION FREQ(250),AMAG(250),PHASE(250),PWR1(250),PWR2(250)
      READ (7,*)
      READ (7,*)
      N=0
100   READ (7,*, END=200,ERR=300) FREQ(N+1), AMAG(N+1), PHASE(N+1)
      N=N+1
      GOTO 100
300   WRITE (1,310) N,FREQ(N),AMAG(N),PHASE(N)
310   FORMAT ('ERROR  ',I5,3F8.2)
      GOTO 500
200   PI=3.14159
      M=N
      DO 400 N=1,M
      PHASE(N)=(PHASE(N))*PI/180.
      VV=10**((AMAG(N)+19.28)/20.)
      PWR1(N)=10.*ALOG10(ABS(1.+VV**2+(COS(PHASE(N))*VV*
     1   2*(1.-8.30E-7*FREQ(N)**2))))
      PWR2(N)=10.*ALOG10(ABS(1.+VV**2+(COS(PHASE(N))*VV*
     2   2*(1.-3.32E-6*FREQ(N)**2))))
400   CONTINUE
      PRINT 110
110   FORMAT ('PLOT=1,CRT=0')
      READ (1,*) IP
      IF (IP.EQ.1) CALL V10U(1,0)
      CALL PLOT2(N,FREQ,PWR1,PWR2,'FREQUENCY~','POWER*DB~')
      IF (IP.EQ.1) CALL V10U(-1,0,'CRPLOT')
500   CONTINUE
      STOP
      END
```

```
C     PROGRAM TO PLOT TOTAL POWER RADIATED BY THREE POINT SOURCES
C     LOCATED 0.1 M APART, COMPARED TO ONE POINT SOURCE
C     HAVING SAME VOLUME VELOCITY.
C     VOLUME VELOCITY AND PHASE OF TWO SOURCES ADJUSTABLE.
      DIMENSION FREQ(200),PWR1(200)
      PRINT 109
109   FORMAT ('ENTER VVC1,VVC2,PSI1,PSI2,R12')
      READ (1,*) VVC1,VVC2,PSI1,PSI2,R12
      DO 100 I=1,200
      FREQ(I)=10**(1.+(FLOAT(I))/100.)
      PWR1(I)=1.+VVC1*VVC1+VVC2*VVC2+VVC1*VVC2*(2.-1.66E-4*(FREQ(I)*
     1   R12)**2)*COS(PSI1-PSI2)+VVC1*(2.-1.66E-6*FREQ(I)*FREQ(I))*
     2   COS(PSI1)+VVC2*(2.-1.66E-6*FREQ(I)*FREQ(I))*COS(PSI2)
      PWR1(I)=10.*ALOG10(ABS(PWR1(I)))
100   CONTINUE
      PRINT 110
110   FORMAT ('1=PLOT, 0=CRT')
      READ (1,*) IP
      IF (IP .EQ. 1) CALL V10U(1,0)
      CALL PLOT(200,FREQ, PWR1,'FREQUENCY~','POWER*DB~')
      IF (IP .EQ. 1) CALL V10U(-1,0,'CRPLOT')
      STOP
      END
```

```
 10  REM NOISE ATTENUATOR SIMULATOR USING TWO CANCELLING LOOPS
 20  DIM R(2,2),S(2,2),G(2,2)
 30  DIM W(1000),X(1000),Y(1000),Z(1000)
 40  DIM V(1000),L(1000)
 50  MAT W=ZER
 60  MAT X=ZER
 70  MAT Y=ZER
 80  MAT Z=ZER
 90  MAT V=ZER
110  MAT S=CON
120  MAT S=(-600)*S
122  DEFINE FILE #1='FFOUT', BIN
124  DEFINE FILE #2='TIME', BIN
130  PRINT 'G(1,1), G(1,2), G(2,1), G(2,2)'
140  INPUT G(1,1),G(1,2),G(2,1),G(2,2)
142  MAT G=(.094)*G
160  PRINT 'INPUT STEP SIZE, LIMIT'
170  INPUT H,M
180  LET C=344.8
190  LET R1=.2
195  LET R2=1
200  LET R3=4
205  LET R4=4.1
210  LET R5=4.2
215  LET R(1,1)=.2
220  LET R(1,2)=1
225  LET R(2,1)=1
230  LET R(2,2)=.2
235  LET D1=INT(R(1,1)/(C*H))
237  LET D2=INT(R(1,2)/(C*H))
239  LET D3=INT(R(2,1)/(C*H))
241  LET D4=INT(R(2,2)/(C*H))
243  LET D5=INT(R1/(C*H))
245  LET D6=INT(R2/(C*H))
247  LET D7=INT(.1/(C*H))
249  LET D8=INT(.11/(C*H))
251  LET D9=INT(.12/(C*H))
252  PRINT D1,D2,D3,D4,D5,D6,D7,D8,D9
254  PRINT 'INPUT STARTING TIME, IMPULSE TIME'
255  INPUT O,N
256  LET V(N)=1/H
258  LET M1=0
259  LET M2=0
260  FOR N=O TO M
261  LET L1=M1
262  LET L2=M2
265  LET A=(W(N-D1))/(R(1,1))
270  LET B=(X(N-D3))/(R(2,1))
275  LET C=(Y(N-D1))/(R(1,1))
280  LET D=(Z(N-D3))/(R(2,1))
285  LET M1=A+B+C+D+(V(N-D5)/R1)
```

```
290  LET A=(W(N-D2))/(R(1,2))
295  LET B=(X(N-D4))/(R(2,2))
300  LET C=(Y(N-D2))/(R(1,2))
305  LET D=(Z(N-D4))/(R(2,2))
310  LET M2=A+B+C+D+(V(N-D6)/R2)
315  LET Q1=3*(G(1,1)*M1+S(1,1)*W(N))-G(1,1)*L1-S(1,1)*W(N-1)
320  LET Q1=W(N)+H*Q1/2
325  LET Q2=3*(G(1,2)*M1+S(1,2)*X(N))-G(1,2)*L1-S(1,2)*X(N-1)
330  LET Q2=X(N)+H*Q2/2
335  LET Q3=3*(G(2,1)*M2+S(2,1)*Y(N))-G(2,1)*L2-S(2,1)*Y(N-1)
340  LET Q3=Y(N)+H*Q3/2
345  LET Q4=3*(G(2,2)*M2+S(2,2)*Z(N))-G(2,2)*L2-S(2,2)*Z(N-1)
350  LET Q4=Z(N)+H*Q4/2
360  LET A=(W(1+N-D1))/(R(1,1))
365  LET B=(X(1+N-D3))/(R(2,1))
370  LET C=(Y(1+N-D1))/(R(1,1))
375  LET D=(Z(1+N-D3))/(R(2,1))
380  LET M3=A+B+C+D+(V(1+N-D5)/R1)
385  LET A=(W(1+N-D2))/(R(1,2))
390  LET B=(X(1+N-D4))/(R(2,2))
395  LET C=(Y(1+N-D2))/(R(1,2))
400  LET D=(Z(1+N-D4))/(R(2,2))
405  LET M4=A+B+C+D+(V(1+N-D6)/R2)
410  LET W(N+1)=G(1,1)*M3+S(1,1)*Q1+G(1,1)*M1+S(1,1)*W(N)
415  LET W(N+1)=W(N)+H*W(N+1)/2
420  LET X(N+1)=G(1,2)*M3+S(1,2)*Q2+G(1,2)*M1+S(1,2)*X(N)
425  LET X(N+1)=X(N)+H*X(N+1)/2
430  LET Y(N+1)=G(2,1)*M4+S(2,1)*Q3+G(2,1)*M2+S(2,1)*Y(N)
435  LET Y(N+1)=Y(N)+H*Y(N+1)/2
440  LET Z(N+1)=G(2,2)*M4+S(2,2)*Q4+G(2,2)*M2+S(2,2)*Z(N)
445  LET Z(N+1)=Z(N)+H*Z(N+1)/2
455  LET L(N+1)=(W(N+1-D7)+Y(N+1-D7))/R3
460  LET L(N+1)=(X(N+1-D8)+Z(N+1-D8))/R4+L(N+1)
465  LET L(N+1)=V(N-D9)/R5+L(N+1)
472  WRITE #1,L(N+1)
474  WRITE #2,(H*N)
480  NEXT N
```

# Appendix 5

## CIRCUIT MODEL

## SOURCE LISTINGS

```
NODES 4
INPUT 1
OUTPUT 4
1 0 R1 1E-3
1 2 R2 7.86E-2
2 3 L1 2.48E-5
3 0 L2 3.45E-4
3 0 C1 1.34E-2
3 0 R3 7.70E-1
3 4 C2 6.74E-4
4 0 R4 1.17E-1
```

Model of experimental loudspeaker.

```
NODES 5
INPUT 1
OUTPUT 5
1 0 R1 1E-3
1 2 R2 7.86E-2
2 3 L1 2.48E-5
3 0 L2 3.45E-4
3 0 C1 1.34E-2
3 0 R3 7.70E-1
3 4 C2 6.74E-4
4 0 R4 1.17E-1
0 5 I5 1 4 0
5 0 R5 1
5 0 L5 6.37E-3
```

Model of loudspeaker and microphone.

```
NODES 8
INPUT 1
OUTPUT 8
1 0 R1 1E-3
1 2 R2 7.86E-2
2 3 L1 2.48E-5
3 0 L2 3.45E-4
3 0 C1 1.34E-2
3 0 R3 7.70E-1
3 4 C2 6.74E-4
4 0 R4 1.17E-1
0 5 I5 1 4 0
5 0 R5 1
5 0 L5 6.37E-3
6 7 I6 1 5 0
6 7 R6 1
7 8 R7 1E3
6 0 R8 1E3
7 0 C7 1.5E-7
6 8 C8 1.5E-7
```

Model of loudspeaker, microphone, and air path.

```
NODES 16
INPUT 1
OUTPUT 15
1 0 R1 1E-3
1 2 R2 7.86E-2
2 3 L1 2.48E-5
3 0 L2 3.45E-4
3 0 C1 1.34E-2
3 0 R3 7.70E-1
3 4 C2 6.74E-4
4 0 R4 1.17E-1
0 5 I5 1 4 0
5 0 R5 1
5 0 L5 6.37E-3
0 6 I6 1 5 0
6 0 R6 1
6 0 C6 0.006
0 7 I7 1 5 0
7 0 R7 1
7 0 C7 0.006
8 9 I8 1 7 0
8 9 R8 1
9 10 R9 1E3
8 0 R10 1E3
8 10 C8 1.5E-7
9 0 C9 1.5E-7
0 11 I11 1 10 0
11 0 R11 1
11 12 R12 2.7E4
11 12 C11 4.7E-9
12 13 R13 2.7E4
13 0 C13 4.7E-8
0 14 I14 1 12 0
14 0 R14 1
14 15 R15 2.7E4
14 15 C14 4.7E-9
15 16 R16 2.7E4
16 0 C16 4.7E-8
```

Model of complete open loop system.

```
NODES 16
INPUT 6
OUTPUT 6
0 1 I1 0 15 0
1 0 R1 1E-3
1 2 R2 7.86E-2
2 3 L1 2.48E-5
3 0 L2 3.45E-4
3 0 C1 1.34E-2
3 0 R3 7.70E-1
3 4 C2 6.74E-4
4 0 R4 1.17E-1
0 5 I5 1 6 0
5 0 R5 1
5 0 L5 6.37E-3
0 6 I6 1 4 0
6 0 R6 1
0 7 I7 1 5 0
7 0 R7 1
7 0 C7 0.006
8 9 I8 1 7 0
8 9 R8 1
9 10 R9 1E3
8 0 R10 1E3
8 10 C8 1.5E-7
9 0 C9 1.5E-7
0 11 I11 1 10 0
11 0 R11 1
11 12 R12 2.7E4
11 12 C11 4.7E-9
12 13 R13 2.7E4
13 0 C13 4.7E-8
0 14 I14 1 12 0
14 0 R14 1
14 15 R15 2.7E4
14 15 C14 4.7E-9
15 16 R16 2.7E4
16 0 C16 4.7E-8
```

Model of complete closed loop system.

Appendix 6

ATTENUATOR SYSTEM

CIRCUIT DIAGRAMS

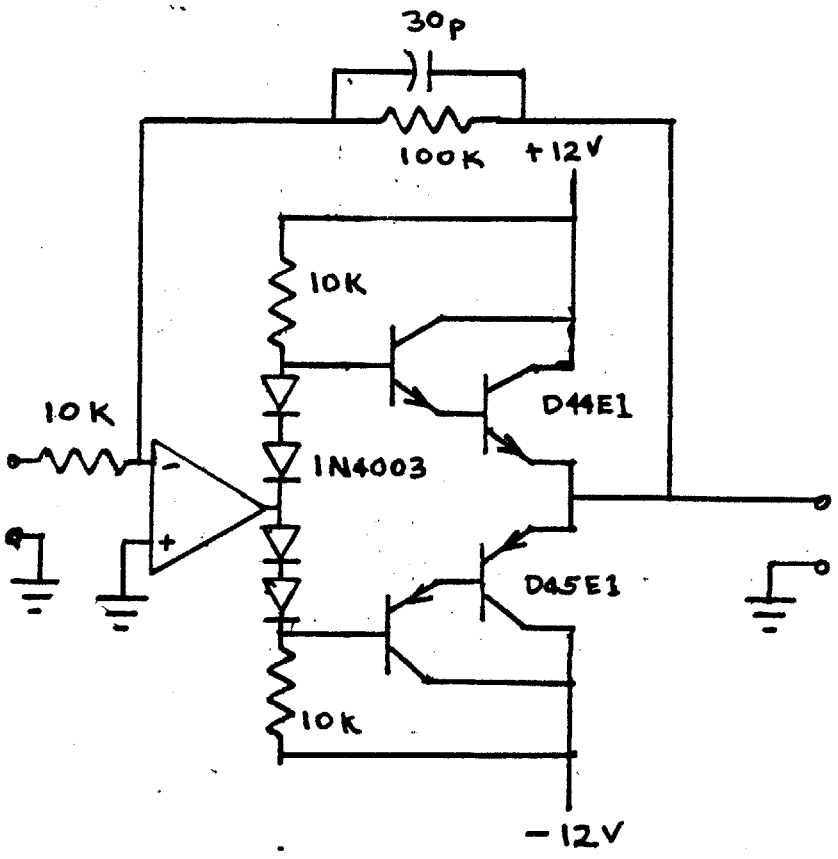


Power amplifier circuit.

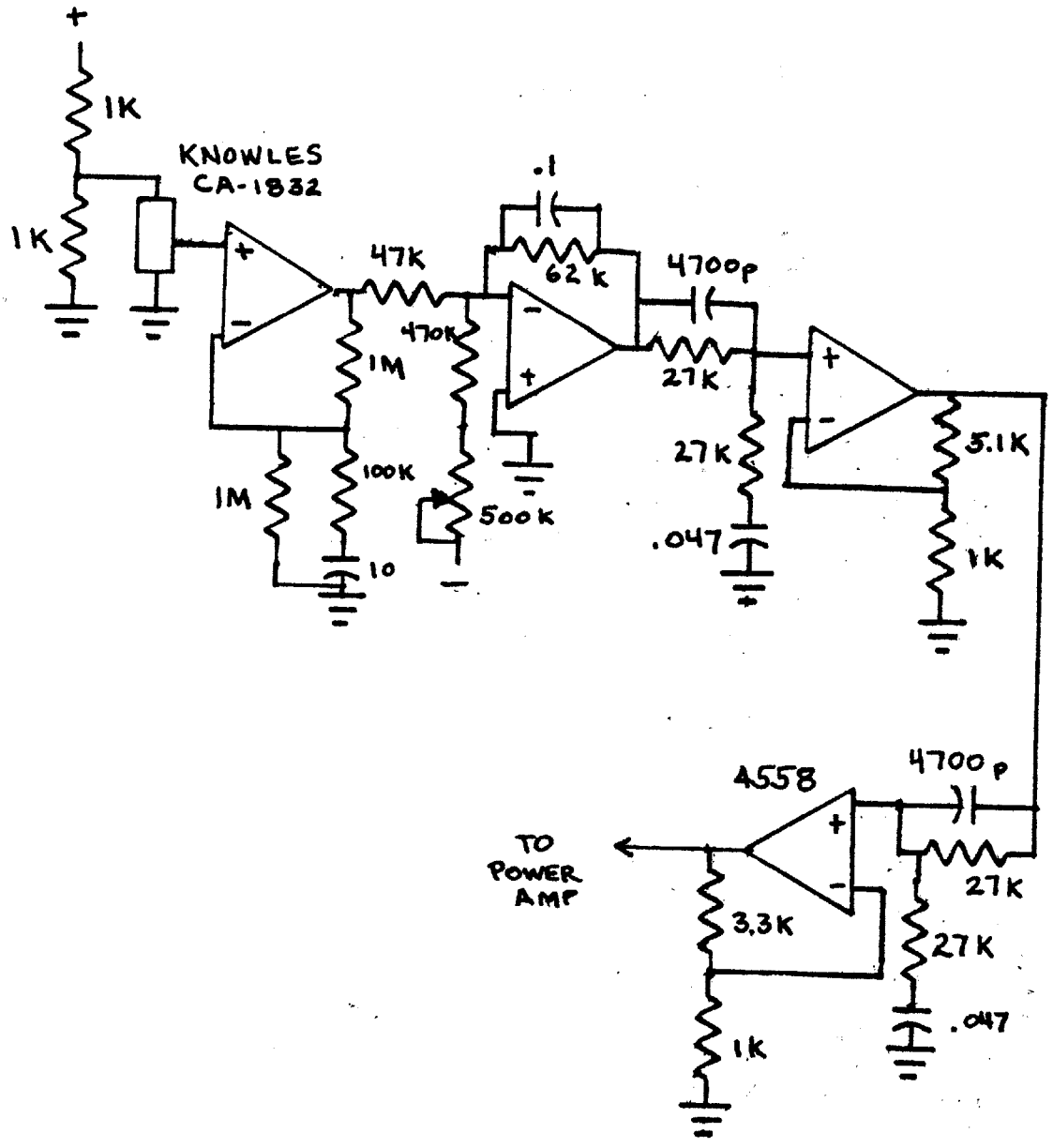


Microphone preamplifier and compensation circuitry.

# REFERENCES

1) L. L. Beranek. Acoustics. New York: McGraw-Hill Book Company. 1954.

2) L. L. Beranek. Noise Reduction. New York: McGraw-Hill Book Company. 1960.

3) G. Canevet. "Active Sound Absorption in an Air Conditioning Duct." Journal of Sound and Vibration 58 (1978): pp 333-345.

4) G. Canevet, and G. Mansiante. "Absorption Acoustique Active et Anti-bruit a une Dimension." Acustica 30 (1974): pp 40-48.

5) L. O. Chua, and P. M. Lin. Computer-Aided Analysis of Electronic Circuits. Englewood Cliffs: Prentice-Hall, Inc. 1975.

6) W. B. Conover. "Fighting Noise by Noise." Noise Control 2 (1956): pp 78-82.

7) A. R. Davidson, and T. G. F. Robinson. "Noise Cancellation Apparatus." U. S. Patent Number 4025724. 1978.

8) E. J. Davison, and S. H. Wang. "An Algorithm for the Calculation of Transmission Zeros of the System (C, A, B, D) Using High Gain Output Feedback." IEEE Transactions on Automatic Control AC-23 (1978): pp 723-740.

9) E. J. Davison, and S. H. Wang. "Properties and Calculations of Transmission Zeros of Linear Multivariable Systems." Automatica 10 (1974): pp 643-658.

10) M. V. Fedoryuk. "An Active Noise-suppresion Method." Soviet Physics Acoustics 20 (1975): p 495.

11) M. E. Hawley. "Acoustic Interference for Noise Control." Noise Control 2 (1956) pp 61-63.

12) M. Jessel, and G. Mansiante. "Active Sound Absorbers in an Air Duct." Journal of Sound and Vibration 23 (1972): pp 383-390.

13) A. S. Knyasev, and B. D. Tartakowski. "Abatement of Radiation from Flexurally Vibrating Plates by Means of Active Local Vibration Dampers." Soviet Physics Acoustics 13 (1967) pp 115-119.

14) A. S. Knyasev, and B. D. Tartakowski. "Vibrational Frequency Characteristics of Bars Constrained by Electromechanical Feedback." Soviet Physics Acoustics 12 (1966): pp 36-41.

15) H. Kwakernack, and R. Sivan. Linear Optimal Control Systems. New York: Wiley Interscience, 1972.

16) J. M. Lawther, and T. H. Rockwell. "Compensation Techniques for Active Damping Improvement." Journal of the Acoustical Society of America 38 (1965): pp 481-482.

17) P. Lues. "Process of Silencing Sound Oscillators." U. S. Patent Number 2043416. 1936.

18) G. Mansiante. "Active Sound Absorption." Journal of the Acoustical Society of America 61 (1977): pp 1516-1523.

19) T. P. McGarty, Jr. "Optimization in a Distributed Acoustic Feedback System." M.S. Thesis, M.I.T. Department of Electrical Engineering. 1966.

20) H. F. Olson. "Control of Noise, Vibration, and Reverberation." Journal of the Acoustical Society of America 28 (1956): pp 966-972.

21) H. F. Olson, and E. G. May. "Electronic Sound Absorber." Journal of the Acoustical Society of America 25 (1953): pp 1130-1136.

22) Y. H. Pao, and V. VaratharaJulu. "Huygens' Principle, Radiation Conditions, amd Integral Formulas for the Scattering of Elastic Waves." Journal of the Acoustical Society of America 59 (1976): pp 1361-1371.

23) J. H. B. Poole and H. G. Leventhall. "An Experimental Study of Swinbanks' Method of Active Attenuation of Sound in Ducts." Journal of Sound and Vibration 49 (1976): pp 257-266.

24) G. Prado. "Observability, Estimation, and Control of

Distributed Parameter Systems." Ph.D. thesis, M.I.T. Department of Electrical Engineering. 1973.

25) T. H. Rockwell, and J. M. Lawther. "Theoretical and Experimental Results on Active Vibration Dampers." Journal of the Acoustical Society of America 36 (1964): pp 1507-1515.

26) E. D. Simshauser and M. E. Hawley. "The Noise Cancelling Headset, an Active Ear Defender." Journal of the Acoustical Society of America 27 (1955): p 207.

27) M. A. Swinbanks. "The Active Control of Sound Propagation in Long Ducts." Journal of Sound and Vibration 27 (1973): pp 411-436.

28) M. A. Swinbanks. "Active Control of Sound Waves." U. S. Patent Number 4044203. 1978.

29) B. D. Tartakowski. "Active Methods for the Compensation of Vibroacoustic Fields." Soviet Physics Acoustics 20 (1975): pp 494-495.

30) W. Tempest. "Loudness and Annoyance due to Low Frequency Sound." Acustica 29 (1973): pp 205-209.

31) P. J. Westervelt. "Absorption of Sound by Sound." Journal of the Acoustical Society of America 59 (1976): pp 760-764.

32) P. J. Westervelt. "Scattering of Sound by Sound." Journal of the Acoustical Society of America 29 (1957): pp 199-203.

33) P. J. Westervelt. "Scattering of Sound by Sound." Journal of the Acoustical Society of America 29 (1957): pp 934-935.

34) A. S. Willsky. "Digital Signal Processing and Control and Estimation Theory -- Points of Tangency, Areas of Intersection, and Parallel Directions." M.I.T. Electronic Systems Laboratory Report 712. 1977.

35) W. A. Wolovich. Linear Multivariable Systems. New York: Springer-Verlag. 1974.

36) W. A. Wolovich and P. Ferreira. "Output Regulation and Tracking in Linear Multivariable Systems." IEEE Transactions on Automatic Control AC-24 (1979): pp 460-465.

# BIOGRAPHICAL INFORMATION

William Rhuel Short was born in 1952, in Syracuse, New York. He lived in a number of towns in the northeast before attending the Massachusetts Institute of Technology. He was awarded the degree of Bachelor of Science in June, 1973, and the Master of Science in June, 1975, both degrees in Electrical Engineering and Computer Science. As a graduate student, Mr. Short assisted with several undergraduate courses, including Acoustics, Linear System Theory, and Semiconductor Device Physics and Circuits. He is a member of Sigma Xi and the IEEE.